TECHNICAL REPORT No. 26

TROPICAL INFLUENCES ON STATIONARY WAVE MOTION IN MIDDLE AND HIGH LATITUDES

by

A. J. Simmons

August 1981

C O N T E N T S

Abstract

The influence of the tropics on the stationary wave motion of middle and high latitudes is examined using idealized model calculations and a preliminary forecast experiment. A steady, linear, primitive equation model is used to illustrate the sensitivity of extratropically-forced wave motion to tropical boundary conditions, and also to examine the extratropical response to tropical forcing. In the latter case an isolated tropical region of diabatic heating may excite a wavetrain with a substantial poleward direction of propagation. The sensitivity of this response is illustrated. Specifying the tropical forcing by means of a relaxation towards climatology results in a large extratropical response.

Barotropic experiments are performed in which an isolated tropical forcing is superimposed on a constant forcing which maintains a climatological basic flow with zonal variation. In these cases a large response is found in the North Pacific region, particularly when the forcing is located to the south of the region of strongest flow. Nonlinearity amplifies or damps this response depending on the sign of the forcing. Maintenance of a region of tropical westerly wind of limited zonal extent results in a substantial cross-equatorial propagation.

The forecast experiment involves comparison of a control forecast with a forecast in which the atmosphere in the tropics is set equal to or relaxed towards analyzed states. The largest high-latitude impact is found for the larger scales of motion in the winter hemisphere, in broad agreement with the results from simpler models.

1. INTRODUCTION

Some of the evidence that the tropics can exert a marked influence on stationary wave motion in middle and high latitudes will be discussed in this report, which comprises a detailed account of material presented at the 1981 ECMWF workshop on 'Tropical Meteorology and its Effects on Medium Range Weather Prediction at Middle Latitudes'. The immediate motivation for this study is a major systematic error of the ECMWF forecast model (and, moreover, of other forecast models), namely a tendency to weaken the major standing-wave pattern in the middle and upper troposphere (Hollingsworth et al, 1980). This error becomes evident, in the mean, before the limit of useful predictability has been reached, and determination of its origin is thus clearly of importance. More generally, interest in the subject of the impact of the tropics on middle latitudes has been stimulated by a growing body of evidence that regions of anomalous heating of the tropical atmosphere, associated with sea-surfacce temperature anomalies, may influence the extratropical standing wave, and thus the seasonal climate.

Attention in this paper will be concentrated largely on results from theoretical and idealized models. The first of two such models examined in detail computes the steady linear primitive-equation response to a steady forcing. Following a brief illustration of the sensitivity to tropical boundary conditions of the extratropical standing wave forced in middle and high latitudes, the model is used to demonstrate the extratropical response to tropical forcing. For an isolated diabatic heating, results obtained (using generally lower model resolution) by a number of authors are reproduced (Egger, 1977; Opsteegh and Van den Dool, 1980; Hoskins and Karoly, 1981; Webster 1981). In addition, a calculation is presented in

which the forcing is given not by an explicit heating, but rather by a relaxation of the steady tropical wave motion towards its climatological distribution.

The second idealized model is a time-dependent, non-linear barotropic vorticity equation model, and forcing is provided by an isolated, steady source of vorticity. Linear results for an extratropical forcing, and a related theoretical examination of wave propagation in a slowly-varying medium, are included in the paper by Hoskins and Karoly (1981). These results are extended here to include the response to an isolated tropical forcing for a basic climatological circulation which varies zonally. It is found that the zonal asymmetry of the basic state results in an enhanced perturbation over the North-East Pacific, an especially large response being found when the forcing is located to the south of the strong Western Pacific jet.

It is important to stress that there is substantial observational evidence, both from case studies (e.g. Bjerknes, 1966, 1969) and from objective studies of many winters (e.g. Horel and Wallace, 1981; Wallace and Gutzler, 1981), and also some evidence from general circulation models (Rowntree 1972, 1976; Julian and Chervin, 1978) which, together with the theoretical and idealized model studies, leads to a reasonably coherent picture of tropical influence on stationary wave motion in middle and high latitudes. This work will not be reviewed here, but towards the end of this paper we will include some results from the first of a series of forecast experiments aimed at quantifying the tropical influence in the context of medium range prediction. In this experiment a standard forecast for the extratropics using the complete global ECMWF model is compared with a forecast in which the model is forced to reproduce uninitialized objective analyses within the tropical belt.

2. THEORETICAL PRELIMINARIES

Many of the model results to be presented in subsequent sections may be explained, at least qualitatively, by the theory of Rossby-wave propagation, and it is thus appropriate to begin with a short account of this theory.

The classical study in this field is that by Charney and Drazin (1961). Although concerned with the vertical propagation of planetary-scale disturbances from the troposphere into the stratosphere and mesosphere, their analysis may also be applied to latitudinal propagation (Charney, 1969). Consider barotropic motion on a latitudinally unbounded β-plane with x and y as eastward and northward coordinates. A steady plane wave perturbation of the form $e^{i(kx+\ell y)}$ to a uniform zonal flow U satisfies the relation

$$\beta - U(k^2+\ell^2) = 0 \qquad (1)$$

If the motion is forced at some fixed latitude with zonal wavenumber k, the meridional wavenumber of the disturbance is given by $\ell^2 = \beta/U-k^2$. The meridional wavenumber ℓ is real, corresponding to wave propagation away from the source, if $\beta/U > k^2$, that is for westerly winds and zonal wavenumbers less than a certain value. For easterly winds, or short zonal wavelengths ℓ is imaginary, and waves are 'trapped', the wave amplitude decaying exponentially away from the source region.

A feature of the primitive-equation solutions discussed in this paper is their approximately barotropic nature in the middle and upper troposphere at latitudes distant from the source region. The likely reason for this may be demonstrated in a simple extension of the above model. We assume

now quasi-geostrophic flow between two rigid horizontal surfaces at z = 0 and z = H, where z is height, and again consider the case of uniform zonal flow.

Away from a source region the boundary conditions of vanishing vertical velocity at z = 0 and z = H imply $\partial\psi/\partial z = 0$ at z = 0, H, where ψ is the perturbation stream function. In this case we find a wave solution of the form

$$e^{i(kx+\ell y)}\, e^{z/2H_s} \left\{\cos mz - \frac{1}{2mH_s} \sin mz\right\} \qquad (2)$$

with

$$\ell^2 = \frac{\beta}{U} - k^2 - \frac{f^2}{4N^2 H_s^2} - \frac{f^2 m^2}{N^2} \qquad (3)$$

and

$$\left(1 + \frac{1}{4m^2 H_s^2}\right) \sin mH = 0 \qquad (4)$$

where f is the Coriolis parameter, N the Brunt-Vaisälä frequency and H_s the density scale height.

Equation (4) has solution $m = \pm i/2H_s$ and $m = \frac{M\pi}{H}$, M an integer. The first solution is identical to the barotropic solution discussed previously, while the other solutions are associated with real m. Inspection of (3) shows these solutions to be associated with a more stringent criterion for latitudinal propagation. Thus far from a source the barotropic component is likely to dominate.

Extension of the above ideas to a vertically-unbounded domain is not straightforward since the wave solution cannot satisfy both the lower boundary condition of either vanishing vertical velocity and the upper boundary condition of either vanishing wave motion or an upward directed energy flux. In particular, inability to satisfy the lower boundary condition rules out a mode with a structure $e^{-mz}\, e^{i(kx+\ell y)}$ which for large enough real m would otherwise yield a latitudinally propagating wave regardless of the direction of the zonal flow.

The assumption of a uniform zonal flow used above for analytical ease is clearly inappropriate for propagating disturbances which extend over a substantial latitudinal range. However, Hoskins and Karoly (1981) have shown that considerable insight into the behaviour of model solutions for latitudinally varying flows may be gained by assuming that the meridional scale of the forced wave varies slowly with latitude. For barotropic motion, the local meridional wavenumber, $\ell(y)$, then satisfies the relation

$$\ell^2 = \frac{\beta_*}{U} - k^2 \tag{5}$$

where U is now the local zonal-mean velocity, and β_* is given by

$$\beta - \frac{d^2 U}{dy^2} \tag{6}$$

for a mid latitude β-plane

or

$$\frac{2\Omega}{a}\cos^3\theta - \cos\theta \frac{d}{dy}\left(\frac{1}{\cos^2\theta}\frac{d}{dy}(U\cos\theta)\right) \tag{7}$$

for spherical geometry, where Ω is the earth's rotation rate, a its radius, and θ is the latitude. The coordinates x and y in this case are derived from a Mercator projection of the sphere

$$x = a\lambda \ , \quad y = a\ell n\{(1+\sin\theta)/\cos\theta\}$$

where λ is the longitude.

From (5) it is seen that propagation occurs over a range of latitudes for which $\beta_*/U > k^2$. Hoskins and Karoly further show, using both standard WKB theory and the concept of conservation of wave action, that the appropriate form for ψ is

$$\psi \ \alpha \ \ell^{-\frac{1}{2}} \exp i\{ kx + \int^{y} \ell dy\} \qquad (8)$$

The $\ell^{-\frac{1}{2}}$ factor represents a variation of wave amplitude as the wave propagates, and in particular, if the wave is excited in a region of large ℓ, its amplitude will increase as it propagates into a region of smaller ℓ. The remote response can thus exceed that near the forcing region, although in more realistic models dissipation may limit the amplitude of this distant response.

Two further points are worthy of note. The first concerns the nature of the wave motion near a latitude where propagation is limited by a small value of β_*, which in several subsequent examples occurs on the poleward flanks of mid-latitude jets. In such regions the WKB solution breaks down, but Hoskins and Karoly show the incident wave to be reflected in this case (see also Geisler and Dickinson, 1974, Lindzen and Tung, 1978). A clear example of this is given subsequently, in Fig. 7.

The second point concerns the singular nature of the steady, linear problem for non-dissipative motion when the zonal-mean flow vanishes at one or more latitudes. In linear, steady-state models aimed principally at studying the forced-wave motion away from singular lines this problem has usually been overcome by inclusion of some form of dissipation which acts mostly in the vicinity of the singular line. Although such models have achieved some success in reproducing gross features of the tropospheric (e.g. Grose and Hoskins, 1979; Fig. 2 of this paper) and stratospheric (e.g. Matsuno, 1970; Simmons, 1978) standing wave structure, results must be viewed with caution in view of a number of non-linear barotropic studies which indicate that non-linear modification of the flow near the zero-wind line may cause significant wave reflection rather than the absorption found in dissipative models. In the quasi-linear model examined by Geisler and Dickinson (1974), the forced wave modified the zonal-mean flow to produce a region of negative absolute vorticity gradient, $\beta - d^2U/dy^2$, which, as noted above, acts to reflect the incident wave. More complete non-linear models (e.g. Stewartson, 1978) confirm this picture, although the non-linear reflection may be weakened by instabilities of the critical layer and by particularly rapid zonal-mean flow changes (Dunkerton et al, 1981). We return to this subject briefly in Section 4.

3. MODELS

In this Section we describe the models used for this study.

a) The linear, steady-state primitive-equation model.

Forced, steady-wave solutions of the linearized primitive equations are determined using sigma-coordinates and a spherical geometry, with the same vertical and meridional finite-difference schemes as in the operational ECMWF model (Burridge and Haseler, 1977). A technique devised by Lindzen and Kuo (1969) is used. Details are given in an Appendix to this paper.

Dissipation is included in the model by means of Newtonian damping and Rayleigh friction with spatially-varying decay rates. It is chosen to represent a boundary-layer drag, a general radiative damping, and an enhanced dissipation in the vicinity of singular lines. The boundary-layer drag corresponds to a decay rate of $(2.5/(5\sigma-4)$ day), $1 > \sigma > 0.8$, while the temperature field is damped at a decay rate which takes the value $(25$ days$)^{-1}$ below 200 mb and increases linearly with the logarithm of pressure to reach a value of $(5$ days$)^{-1}$ at 1 mb. Singular-line dissipation is included by increasing the above rates to $(2(\bar{u}/\cos\theta)^2$ day$)^{-1}$, where $\bar{u}$ is the zonal mean flow in ms^{-1}, wherever they fall below this value. Since the total wavenumber, according to linear barotropic theory, varies approximately as the inverse square root of $\bar{u}$, this latter dissipation is likely to be approximately equivalent to a fourth-order linear diffusion with constant coefficient, as used, for example, in Hoskins and Karoly's (1981) study.

A weakness of this model is the absence of any parameterization of the effect of transient disturbances on the forced wave motion. The extent to which such disturbances may also act to dissipate larger scales is unclear. Lau (1979) demonstrated a strong tendency for the heat transports

by transient eddies to destroy the zonally asymmetric component of the stationary temperature field, but conversely, Lau and Wallace (1979) indicated that the transient eddies may act as a forcing of the time-averaged asymmetries of vorticity. It is likely, however, that the lack of any representation of transient effects is responsible for the relatively weak surface features found (but not illustrated here) with this model.

All calculations to be presented use the same vertical and meridional resolution as in the operational version of the ECMWF model. They are thus of global extent with a latitudinal grid spacing of 1.875°. Fifteen levels are used in the vertical, with a top level at σ = .025. Tests with substantially higher top levels gave very similar results, although they should be treated with caution as all calculations appeared to underestimate vertical propagation compared with climatology. The zonal resolution comprises wavenumbers up to six, since limited tests showed no significant differences to result from inclusion of higher wavenumbers.

Zonal-mean states for use in this model were obtained by interpolating zonally-varying pressure-level climatologies (originally made available by the National Center for Atmospheric Research, USA) to the model sigma levels, assuming no orography. Zonal means were then taken on the sigma surfaces. The resulting surface flows were found, in middle latitudes, to be some two thirds the strength of corresponding flows computed from a sigma-coordinate climatology with the full earth orography.

b) The barotropic model.

This model uses a spectral representation and is a barotropic version of the multi-level model described by Hoskins and Simmons (1975). For these calculations a global version, with triangular truncation of the spectral

expansion at total wavenumber 42 and a timestep of 30 min, was used. Repetition of a sample calculation using a wavenumber 21 truncation gave very similar results, apart from slightly reduced amplitude maxima. A linear drag with a decay rate of $(14 \text{ days})^{-1}$ and a fourth order linear diffusion with a coefficient of 2×10^{16} $m^4 s^{-1}$ were included. Comparison with a calculation in which these dissipations were set to zero showed similar qualitative results, but amplitudes were some 70% larger at day 10 in the undamped case.

Spectral climatological vorticity fields for use as initial conditions for this model were derived by applying a modified form of the ECMWF operational post-processing to sigma co-ordinate, grid-point climatologies.

c) The forecast model.

The forecast experiments used the operational ECMWF model (Burridge and Haseler, 1977; Tiedtke et al, 1979). The first experiment was a standard forecast from the FGGE III-b initialized analysis for 12 GMT, 11 June 1979. The second experiment was identical to the first apart from the fact that, at latitudes between 30°N and 30°S, each forecast quantity, x say, was modified at the end of each timestep according to the formula $x = ax_{analysis} + (1 - a)x_{forecast}$ where $x_{analysis}$ represents the value of x derived by linear interpolation using uninitialized FGGE analyses available at 6-hourly intervals, and $x_{forecast}$ represents the forecast value. Uninitialized values were chosen in view of the suppression of tropical divergences caused by the initialization technique employed in the production of the analyses. The value of a varied with latitude approximately according to the formula

$$\tfrac{1}{2}(1 + \tanh 20(\theta_{\frac{1}{2}} - \theta))$$

where θ is the latitude in radians and $\theta_{\frac{1}{2}} = 25.3125\pi/180$, giving values a = .123 at model latitude 28.125° and a = .658 at latitude 26.25°.

4. TROPICAL INFLUENCES ON THE EXTRATROPICAL RESPONSE TO EXTRATROPICAL FORCING

Our first example of the way the tropics can affect the extratropical standing wave pattern concerns the influence of the tropics on the response to steady orographic and thermal forcing in middle latitudes. Specifically, we compare two linear, steady-state solutions which have the same extratropical forcing, but a different treatment of the tropics.

The zonal mean state for these calculations is that based on the climatology for January. An idealized thermal forcing which decreases with height as σ^2 and whose surface distribution is shown in Fig. 1 is used. The orographic forcing uses the distribution of orography currently used operationally at ECMWF, but amplitudes are multiplied by a factor 1.5. This enhancement was chosen principally to ensure an extratropical response of realistic magnitude, although it may be justified qualitatively by noting that the orographic forcing is likely to be underestimated in linear calculations such as these since vertical motion is forced by the impact of a relatively weak sea-level zonal flow on the mountain slopes.

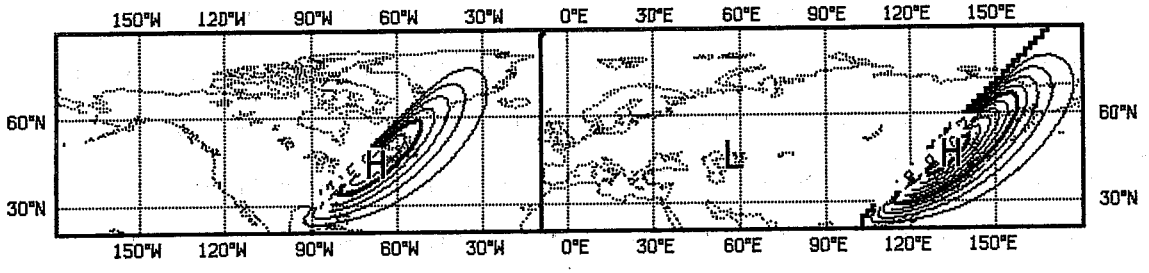

Fig. 1 An idealized distribution of diabatic heating. The contour interval is 1°C/day.

The first of the two solutions was obtained using the standard model described in the preceding section. In this case a dissipative critical latitude where the zonal-mean flow vanishes exists at all levels in the tropics. In the second solution, the motion was confined north of model latitude 14.0625°N where the reflecting boundary condition v=0 was applied. At this latitude the zonal-mean wind is westerly between about 600 and 50 mb. Since the first solution is changed little by removing the orographic forcing south of 15°N, the difference between these solutions illustrates the sensitivity of results to the representation of the tropics as a boundary condition on the wave motion forced in middle latitudes.

Geopotential fields at 500 mb are compared in Fig. 2. Also shown, for reference, is the climatological field for January. It is clear that while both model solutions provide a reasonable representation of climatology, there are, nevertheless, quite large differences between them. Not surprisingly, wave amplitudes are generally larger in the case of the reflecting boundary condition, and the flow patterns resemble those of blocking situations, as has been suggested by Tung (1979) and Tung and Lindzen (1979) in the case of a reflecting critical latitude.

The linear, steady-state model does not yield a representation of climatology sufficiently accurate to favour one or other of the solutions discussed above, particularly in view of the rather arbitrary enhancement of the height of the orography noted earlier. These solutions do, however, suggest that for accurate numerical simulation of the extratropical standing wave pattern it is important to represent the effects of the tropical critical latitude. The accuracy with which such effects are currently treated in numerical models is far from clear, partly because of the theoretical uncertainty concerning the precise nature of these effects, and partly because of the many other interacting sources of error in numerical models.

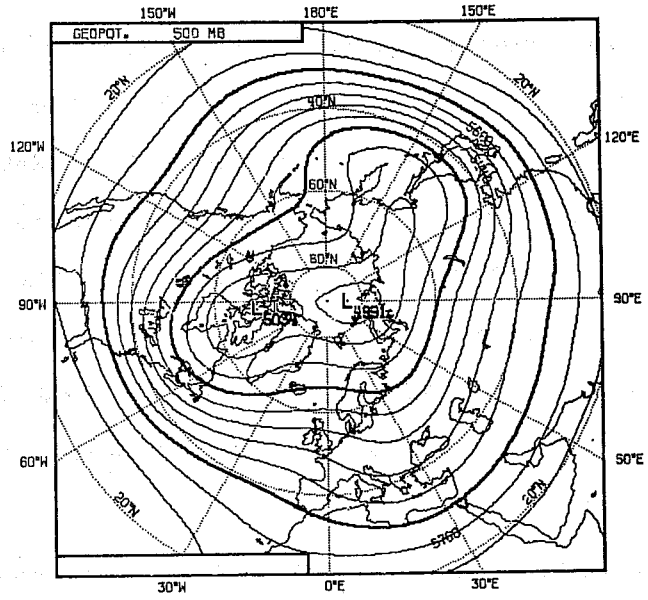

January climate

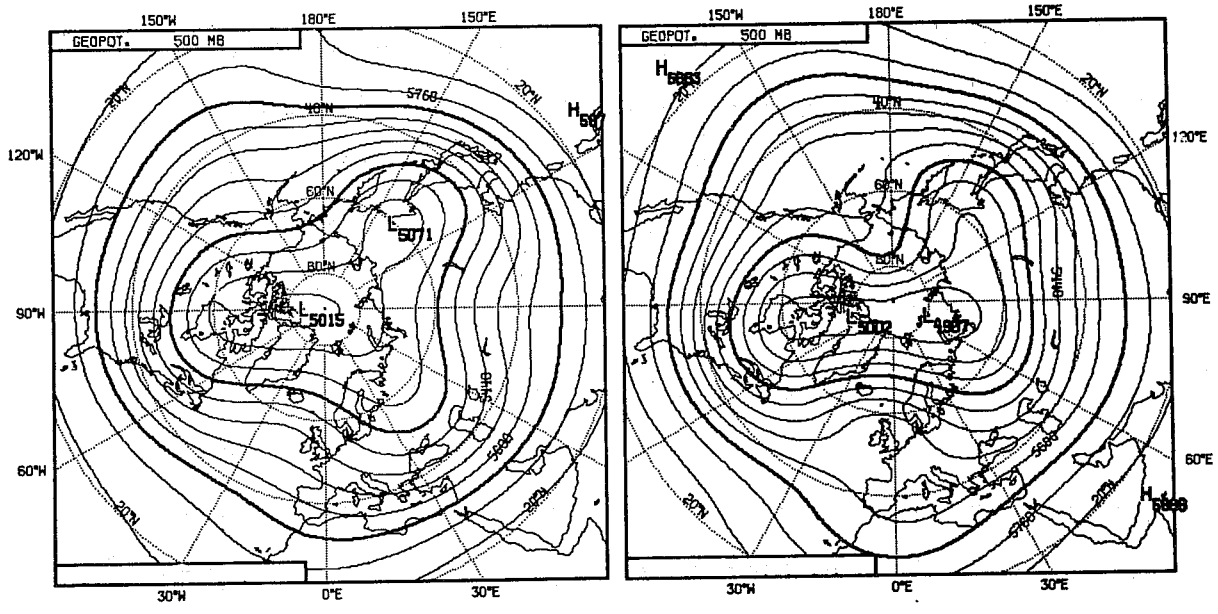

Global model

v = 0 at 14°N

Fig. 2 The climatological mean 500 mb geopotential for January (upper) and for calculations using a global model (lower left) and a model with a reflecting boundary condition at the model latitude close to 14^{o}N (lower right). The contour interval is 8 dam.

5. THE EXTRATROPICAL RESPONSE TO AN ISOLATED REGION OF DIABATIC HEATING

For these calculations we again use the linear, steady-state model, but we now consider the case in which the only forcing is provided by an isolated region of heating located within the tropical atmosphere. Reference has been made in the introduction to a number of similar previous studies and the discussion presented here should be regarded in part as reviewing the results of these studies, although the present results are novel in that they use a substantially higher computational resolution. This type of calculation has usually been performed in order to assess the influence of tropical sea surfacce temperature anomalies on middle latitudes, but it is of equal relevance to the question of the extent to which the climatological extratropical standing wave pattern may be forced by geographical variation in the time-mean level of convective activity in the tropics.

The horizontal variation of the diabatic heating, Q, is given by the zonally non-uniform part of the function

$$\begin{cases} \left(\sin \dfrac{\pi(\theta-\theta_1)}{(\theta_2-\theta_1)} \sin \dfrac{\pi(\lambda-\lambda_1)}{(\lambda_2-\lambda_1)} \right)^2 & , \lambda_1 < \lambda < \lambda_2,\ \theta_1 < \theta < \theta_2, \\ 0 \text{ otherwise} \end{cases} \tag{9}$$

This is illustrated in Fig. 3 for the values $\lambda_1 = 90°$, $\lambda_2 = 180°$, $\theta_1 = 0°$, $\theta_2 = 30°$, which are used as standard unless otherwise stated. Although the absolute value of the longitudes is of no significance in these calculations involving a zonal-mean basic state and no orographic forcing, all maps will be presented for the forcing centred at 135°E and will include a representation of the coastlines in order to give some idea of the spatial scale of the response.

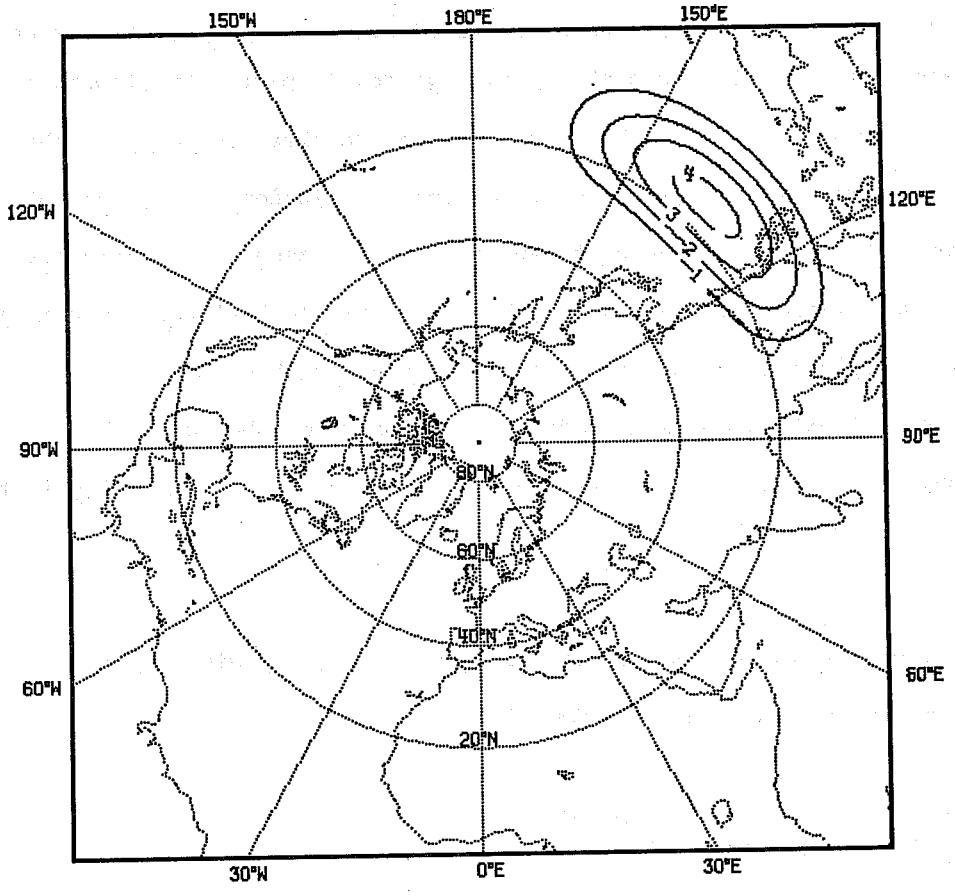

Fig. 3 The horizontal distribution of diabatic heating given analytically by Eqn.(9) with a maximum value of 5 units.

Results have been obtained for a number of vertical distributions of Q, some of which are shown in Fig. 4. That used for most calculations has a maximum at 400 mb, and is shown in Fig. 4a. It should be noted that since the calculations are linear the amplitude of the response is simply linearly proportional to the amplitude of the heating. The results presented subsequently are all for a relatively large heating maximum of 5°C/day.

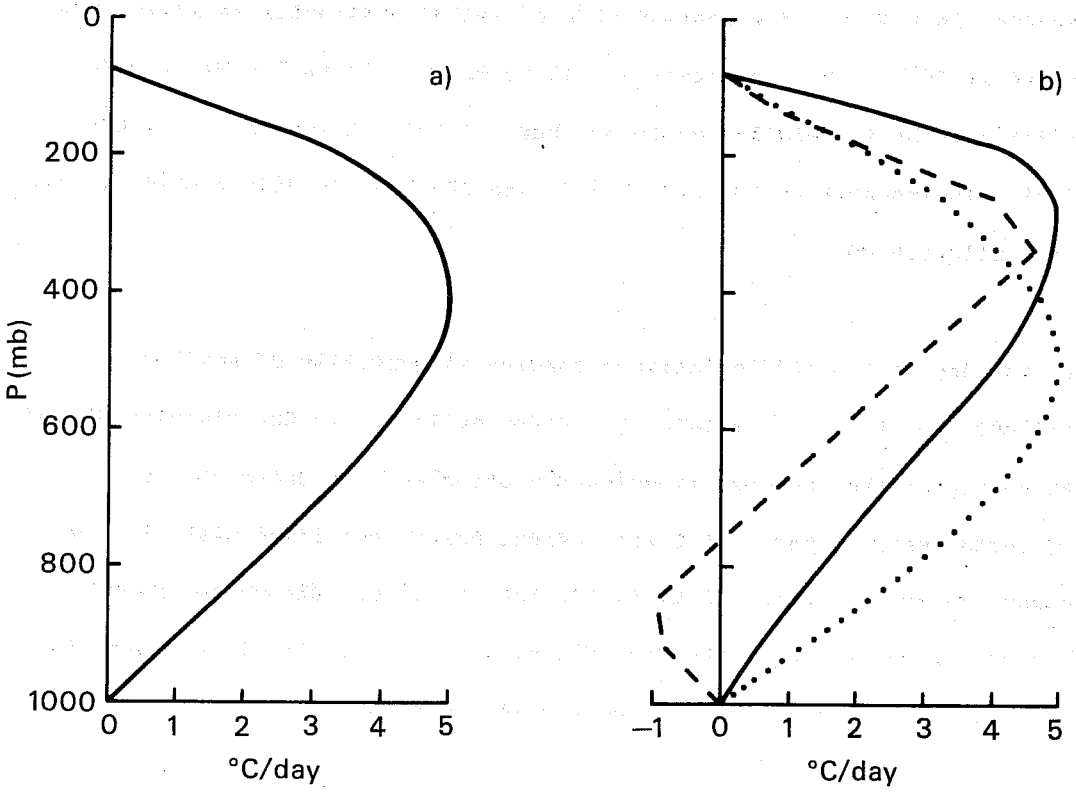

Fig. 4 Vertical distributions of diabatic heating.

The perturbation geopotential field at various levels is shown in Fig. 5 for the January climatological zonal-mean state and for the standard forcing shown in Figs. 3 and 4a. The isolated region of tropical heating evidently excites, in this case, a substantial extratropical response which appears as a train of waves with a substantial poleward as well as zonal direction of propagation. The barotropic nature of the extratropical response is also evident, the wave pattern being largely independent of height apart from an intensification of the Aleutian anticyclone at stratospheric levels.

It is of interest to compare the results shown in Fig. 5 with those presented in Fig. 6 for a heating with a similar horizontal variation but centred at 45°N. In this case the heating maximum is at 700 mb, a more realistic value for middle latitudes, but the qualitative nature of the solution is insensitive to this choice, and the heating distribution itself is not illustrated.

The response to the middle-latitude forcing is generally of smaller amplitude than that to the forcing centred at 15°N. In the vicinity of the heating region the response is evidently baroclinic in character, a pronounced westward phase tilt with height being associated with the low pressure centre which at 700 mb is located at 150°E. Elsewhere, however, the vertical variation of the forced wave is small, as is clearly seen in the low centred to the north of the American continent.

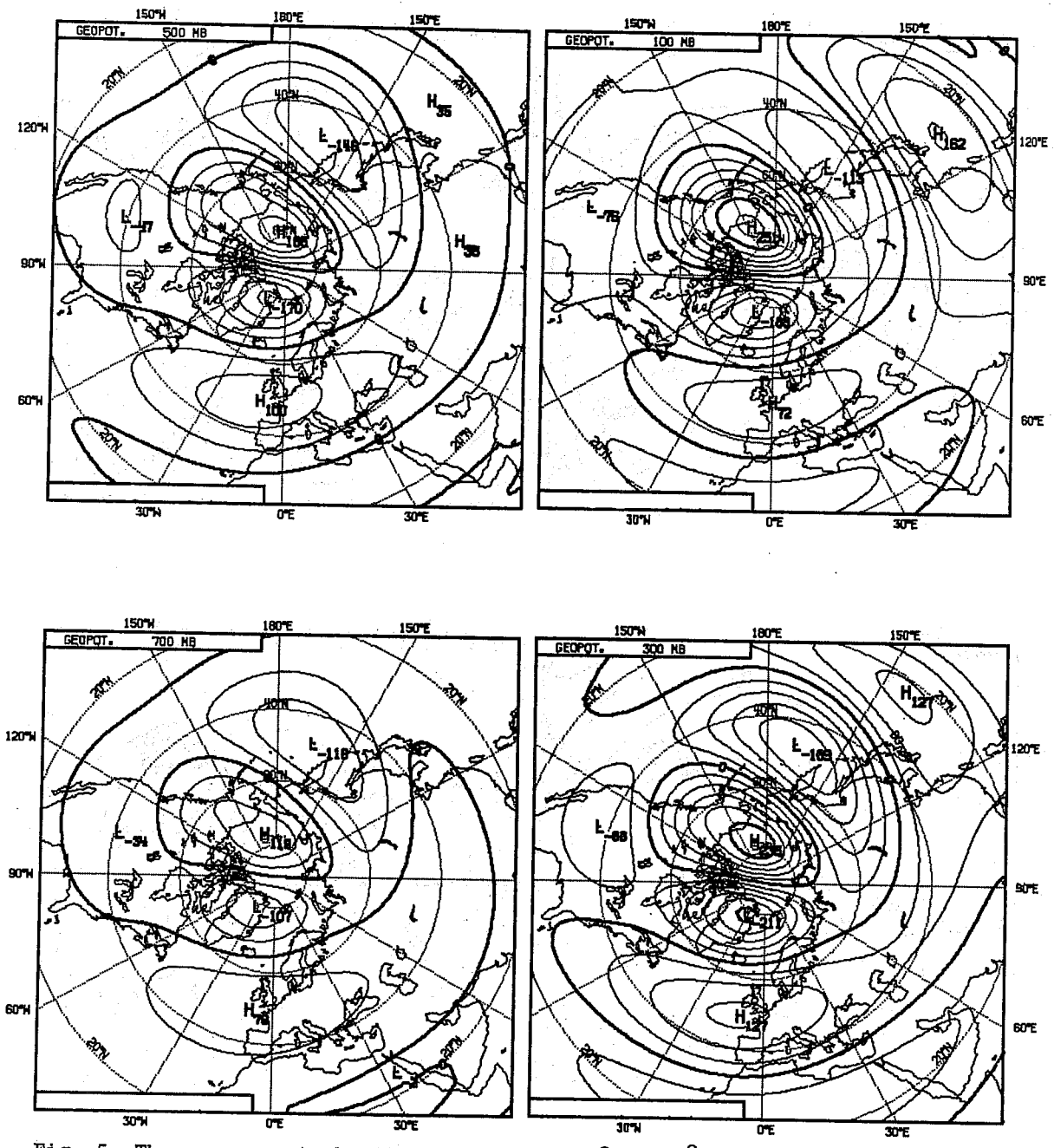

Fig. 5 The response to heating centred at 15°N, 135°E. The perturbation geopotential is shown at 700 mb (lower left), 500 mb (upper left), 300 mb (lower right) and 100 mb (upper right). The contour interval is 4 dam.

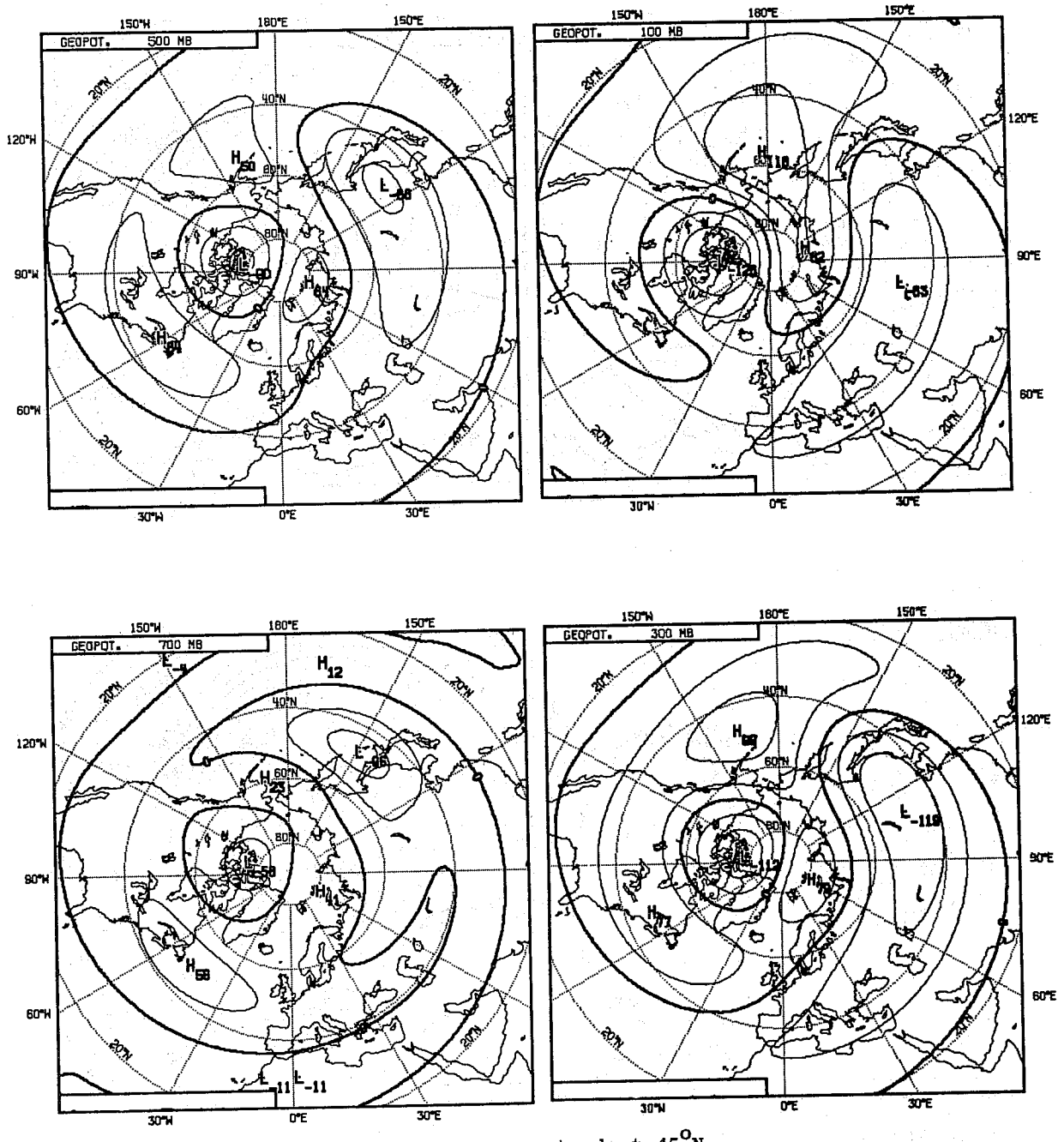

Fig. 6 As Fig. 5, but for a heating centred at 45°N.

The extratropical response to the tropical forcing is found to be highly sensitive to the zonal-mean state. This is illustrated by Fig. 7. For the July climatological state the forcing centred at 15°N is located almost entirely within a region of easterly flow, and a very small response is found at middle and high latitudes. Less seasonal variability occurs in the Southern Hemisphere response to a forcing centred at 15°S, and there is also in these cases an inhibition of the cross-polar propagation evident for the Northern Hemisphere. Instead, there is a clear zonal and then equatorward direction of propagation of the wave train.

The latter result may be readily understood in terms of the ray theory developed by Hoskins and Karoly (1981). The zonal-mean jet in the southern hemisphere possesses stronger meridional vorticity gradients than the northern hemisphere jet, and even for the climatological mean state the poleward gradient of absolute vorticity becomes negative on the poleward flank of the jet. As discussed in Sect. 2, propagating disturbances of all zonal scales may thus be expected to be reflected away from this latitude in agreement with the picture shown in the lower half of Fig. 7. It should also be noted that since climatological vorticity gradients are inevitably smaller than day to day values it is likely that similar results may commonly hold for actual propagation in the northern hemisphere.

The amplitude and pattern of the forced wave motion is also sensitive to the latitude of the maximum forcing. The weaker response to a middle-latitude forcing has already been noted, while Fig. 8 shows that for the January mean state amplitudes are some 50% weaker for forcing at 5°N and 25°N than for the 15°N forcing discussed earlier. Substantial differences in phase are also evident. The region of equatorial easterlies ensures a negligible northern hemisphere response for a forcing centred at 15°S.

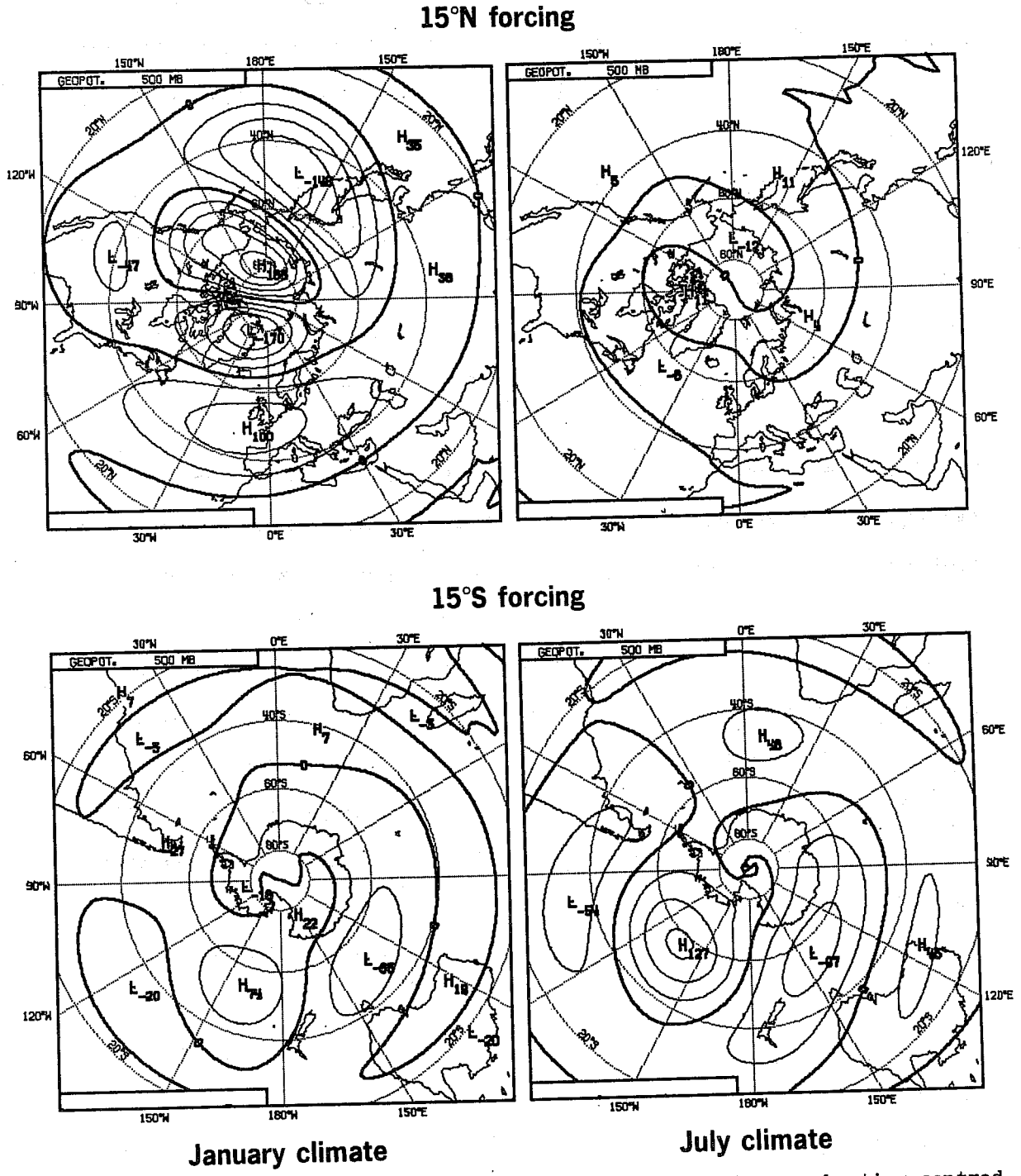

Fig. 7 The 500 mb response for the Northern Hemisphere (upper, heating centred at 15°N) and the Southern Hemisphere (lower, heating centred at 15°S). Results are presented for January (left) and July (right) climatological mean flows.

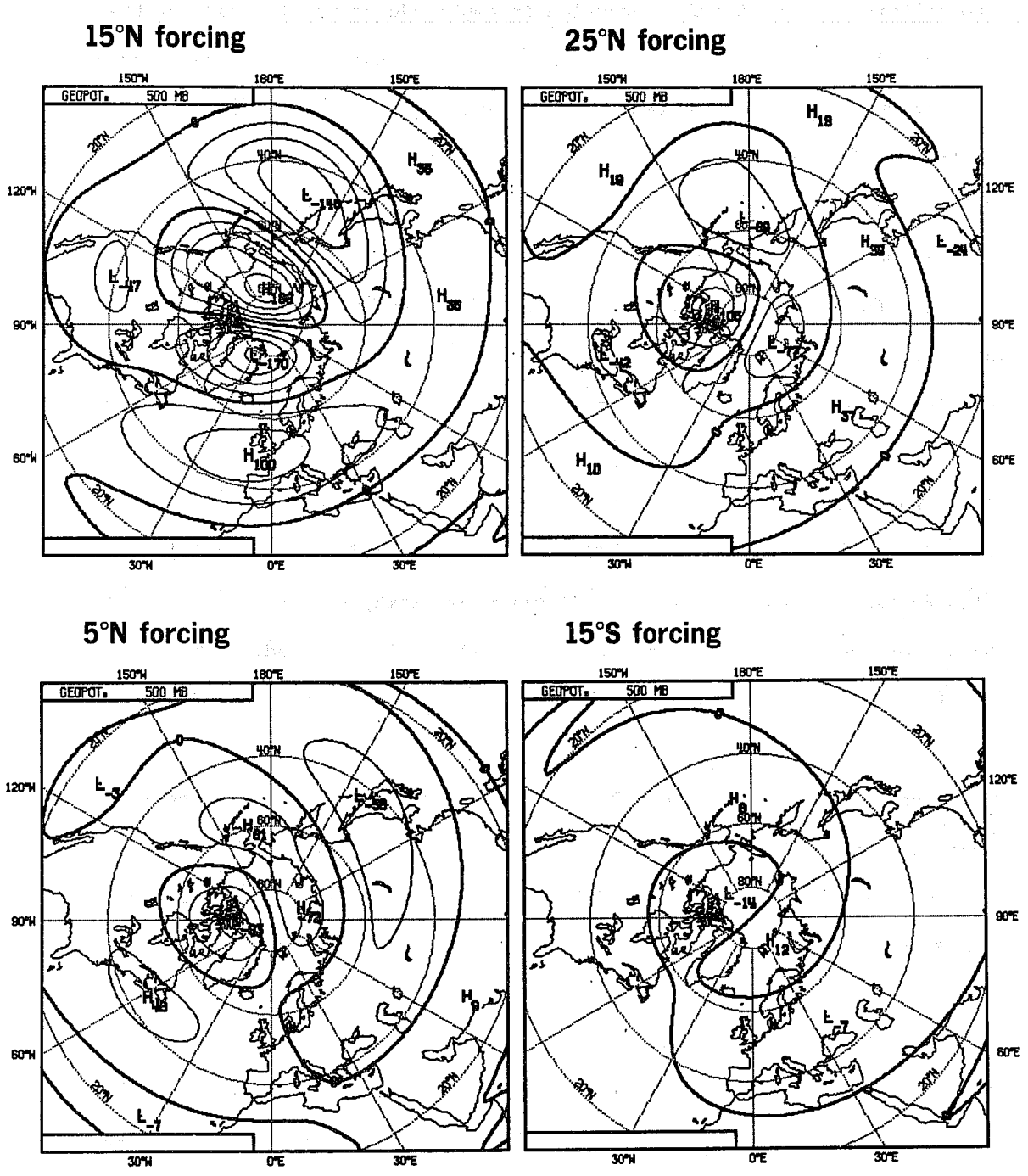

Fig. 8 500 mb height perturbations for heatings centred at 135°E and various latitudes.

Two factors account for the reduction in amplitude as the latitude of the tropical forcing decreases. The first is that an increasing amount of the forcing region lies in the region of easterly wind which acts to trap stationary disturbances. The second is associated with the nature of the forcing of the wave motion. Locally, the tropical diabatic heating is largely balanced by vertical motion, as indicated by a standard scale analysis (see, for example, Holton 1979). The associated vorticity generation decreases with the Coriolis parameter as the latitude of maximum heating is moved towards the equator.

Other sensitivity studies have been performed. Fig. 9 compares results for the 15°N forcing and the four different vertical profiles of heating illustrated in Figs. 4a) and b). Little sensitivity to variations in the height of the heating maximum from 300 to 500 mb is revealed. Similar results are found for distributions of heating centred at 5° and 25°N.

This insensitivity to the detailed vertical structure of the heating is consistent with the equivalent barotropic structure of the forced wave motion. Given that the perturbation stream function may be approximated by the form

$$\psi = A(z)\ \phi(x,y) \tag{10}$$

the forcing term $\frac{f^2}{\rho_o}\frac{\partial}{\partial z}\left(\frac{\rho_o Q}{N^2}\right)$ in the quasi-geostrophic potential vorticity equation may be split into a term proportional to A(z) and a remainder orthogonal to A(z). The relevant component proportional to A(z) depends on Q through an integral

$$\int_o^\infty A(z)\ \frac{1}{\rho_o}\ \frac{\partial}{\partial z}\left(\frac{\rho_o Q}{N^2}\right) dz$$

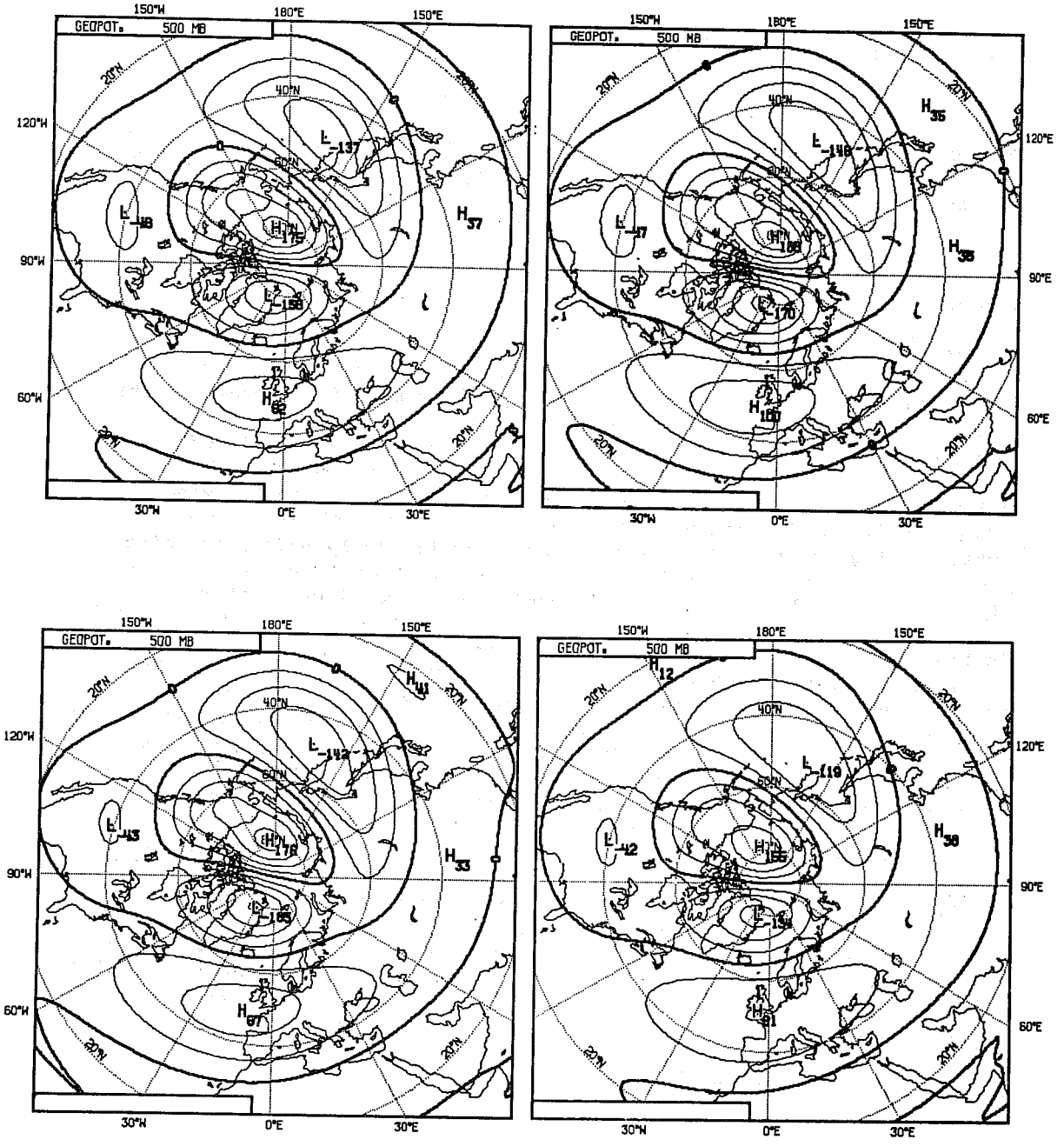

Fig. 9 The 500 mb response to the vertical distributions of heating shown in Fig. 4. The upper plots are for the two heatings represented by solid lines, with maxima at 300 mb (left) and 400 mb (right), while the lower plots are for the heating maximum at 500 mb (left) and the second profile with a 300 mb maximum (right).

which, if Q vanishes at z=0 and as $z \to \infty$ may be written

$$-\int_0^\infty \frac{\rho_o Q}{N^2} \frac{\partial}{\partial z}\left(\frac{1}{\rho_o} A(z)\right) dz$$

The effective forcing thus depends on a weighted vertical integral of the heating, and may be insensitive to its detailed vertical structure.

Consequences of varying the horizontal distribution of heating are illustrated in Figs. 10 and 11. Fig. 10 shows results to be highly insensitive to reducing or increasing by 50% the meridional scale of the forcing region, while, conversely, Fig. 11 shows the amplitude of the polar response to be approximately linearly proportional to the zonal extent of the forcing. The latter result may be easily understood since the solution in the polar region is dominated by zonal wavenumber one, and is thus approximately proportional, in this linear calculation, to the zonal wavenumber one component of the tropical heating, which increases as the zonal scale of the heating increases. The former result arises partly because of a tendency, in the case of a forcing of larger latitudinal extent, for cancellation between the components of the solution forced by the heating near the northern and southern boundaries of the forcing region. This may be seen by referring back to Fig. 8, which shows the high latitude response to forcings centred at 5° and 25°N to be of similar amplitude, but almost completely out of phase.

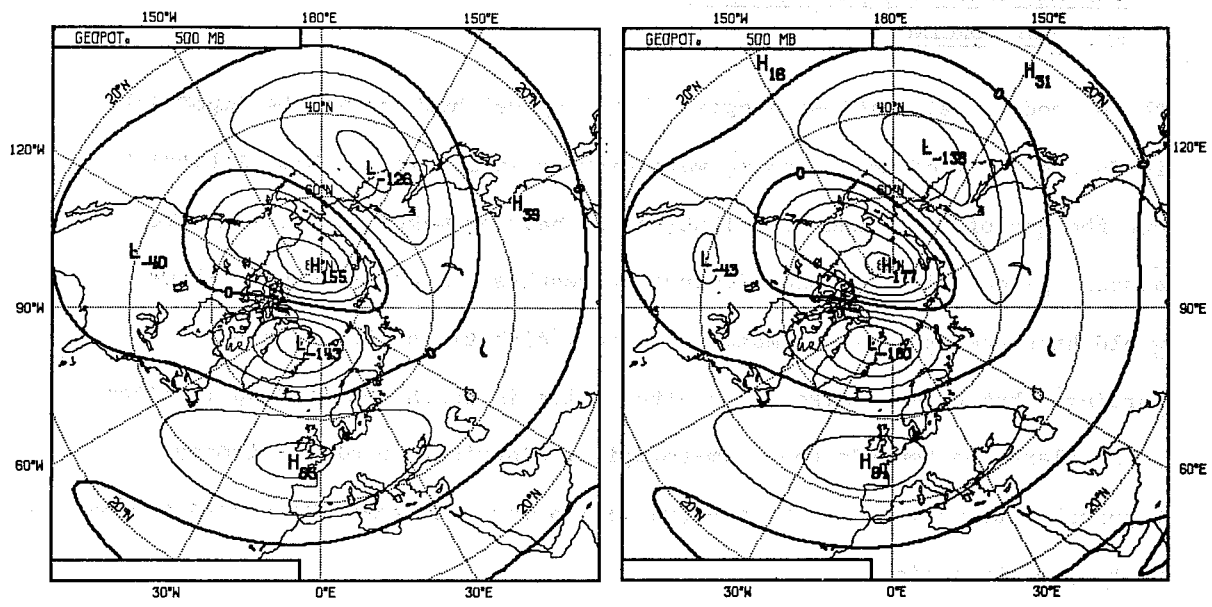

Fig. 10 As Fig. 5 for the 500 mb level, but for heating distributions with a meridional scale 50% smaller (left) and 50% larger (right).

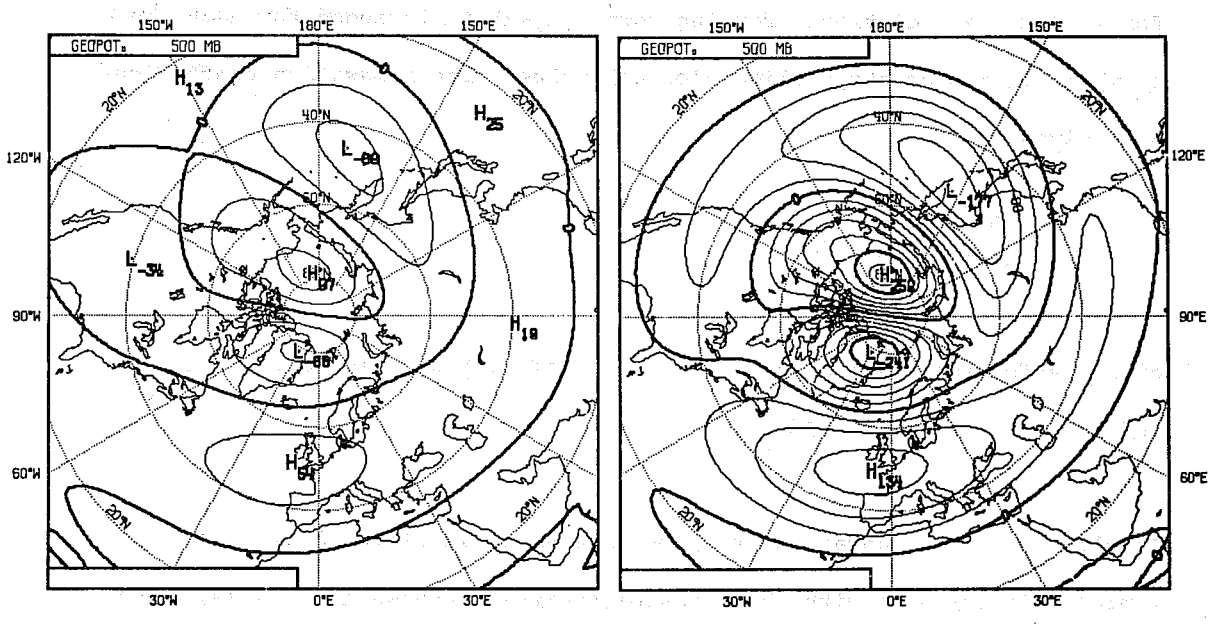

Fig. 11 As Fig. 5 for the 500 mb level, but for heating distributions with a zonal scale 50% smaller (left) and 50% larger (right).

6. THE RESPONSE TO CLIMATOLOGICAL TROPICAL FORCING

The preceding calculations suggest that tropical heating may be important in forcing part of the standing wave pattern in middle and high latitudes, but the use of idealized distributions of heating makes it difficult to assess the quantitative significance of results. A possible next stage would have been to use estimates of actual diabatic heating rates as forcings, but here we discuss an alternative in which the forcing is given by a relaxation towards the climatological distribution of stationary tropical wave motion, which is known more accurately than the corresponding heating distribution.

The relaxation is included in the linear steady-state model in the following way. The equations north of latitude θ_2 are unchanged. South of latitude θ_1 all fields are set equal to their climatological value, while for $\theta_1<\theta<\theta_2$ an additional forcing term $\chi(x_i-x)$ is included for each field x, where x_i represents a climatological value. The relaxation coefficient χ is given by

$$\chi = \left(\frac{\theta_2-\theta}{\theta_1-\theta}\right)^2 \quad \text{day}^{-1}$$

giving e-folding times of 9 days for $\theta = (3\theta_2+\theta_1)/4$, 1 day for $\theta = (\theta_1+\theta_2)/2$ and 1/9 day for $\theta = (\theta_2+3\theta_1)/4$.

Results using the January climatology are shown in Fig. 12 for $\theta_1=10°$ and $\theta_2=30°$. Comparisons with the climatology itself (shown in Fig. 13) shows the tropical forcing to excite a middle and high latitude response which is of an amplitude comparable to that of the climatological standing wave. The tropical forcing evidently (and not surprisingly) does not account for all features, in particular the East Asian/West Pacific trough, but some aspects of the solution are in remarkable agreement with climatology,

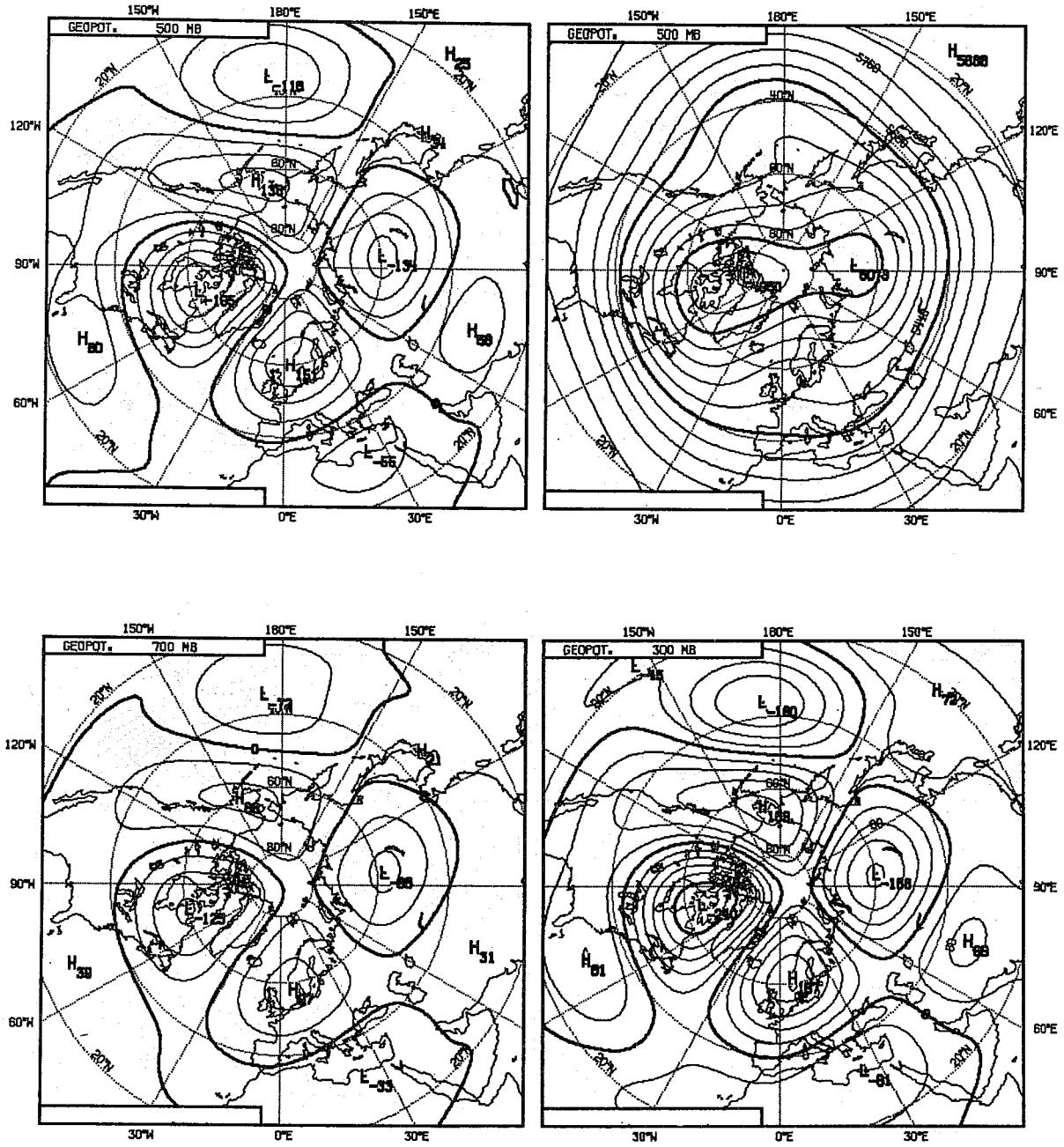

Fig. 12 The extratropical response forced by a relaxation towards the January tropical climatology. Perturbation geopotentials are plotted with a contour interval of 4 dam at 700 mb (lower left), 500 mb (upper left) and 300 mb (lower right). The total 500 mb field (contour interval 8 dam) is also shown.

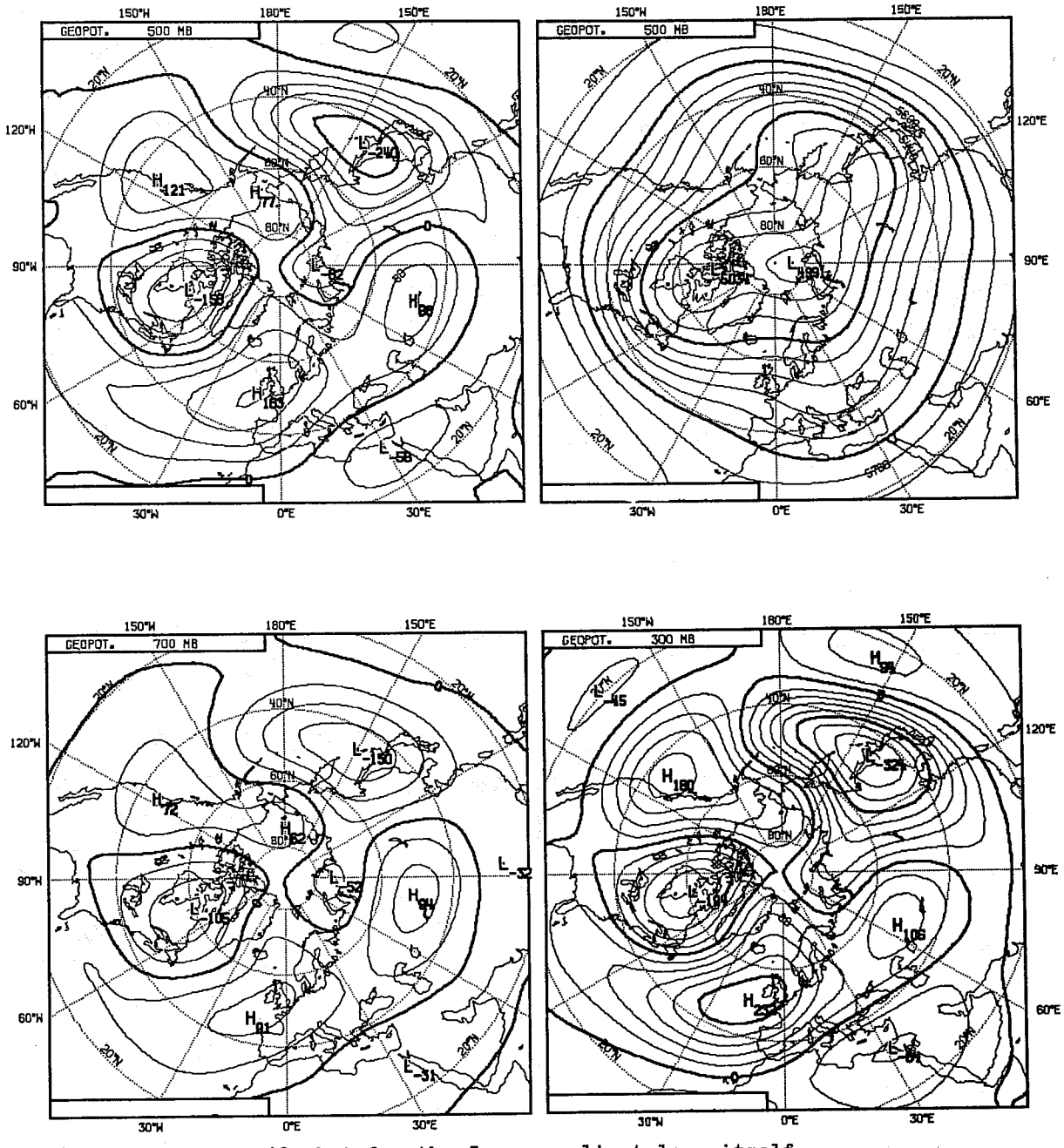

Fig. 13 As Fig. 12, but for the January climatology itself.

notably the North American trough. The absence of any substantial phase tilts in the vertical between 700 and 300 mb is a feature of the climatological pattern which is also worth noting.

It is important to stress that these model results must be treated with caution. Reducing the width of the relaxation zone by setting $\theta_1 = 17.5^\circ$ and $\theta_2 = 22.5^\circ$ gives a response with a very similar pattern to that shown in Fig. 12, but amplitudes are generally some 40% larger. The solution for $\theta_1 = 5^\circ$ and $\theta_2 = 25^\circ$ (Fig. 14) is generally similar, but somewhat poorer in its representation of the North American trough. Uncertainties over the level of dissipation and parameterization of transient wave effects also make quantitative assessment difficult, but we may nevertheless conclude that it is likely that a realistic representation of the effects of tropical forcing is required in forecast and general circulation models for accurate simulation of the extratropical standing wave pattern. A more definite conclusion must await further studies.

7. EFFECTS OF TRANSIENCE, ZONALLY NON-UNIFORM BASIC FLOWS AND NON-LINEARITY

7.1 Introduction

The barotropic model described in Sect. 3b is used for this particular aspect of our study. Initial conditions (illustrated in Fig. 15 for the 300 mb level in January) comprise either a zonal mean or a zonally-varying climatological basic flow, and in the latter case a constant vorticity forcing is included to keep the basic flow constant in time. An additional vorticity forcing is initiated over an isolated tropical region at $t = 0$. The former forcing is viewed as representing the climatological forcing of the standing wave pattern by orographic and thermal effects and by interactions with transient disturbances. The additional isolated forcing is viewed as the effect of a region of anomalous tropical heating.

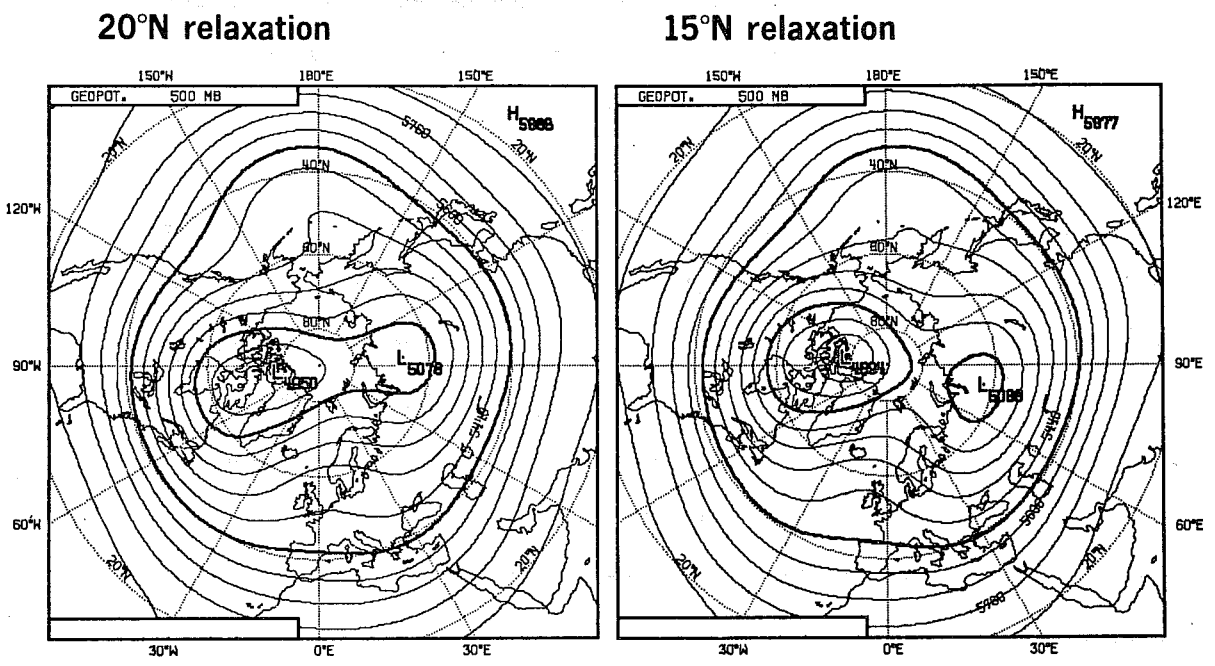

Fig. 14 The 500 mb height fields forced by relaxations to tropical climatology centred at 20°N (left) and 15°N (right).

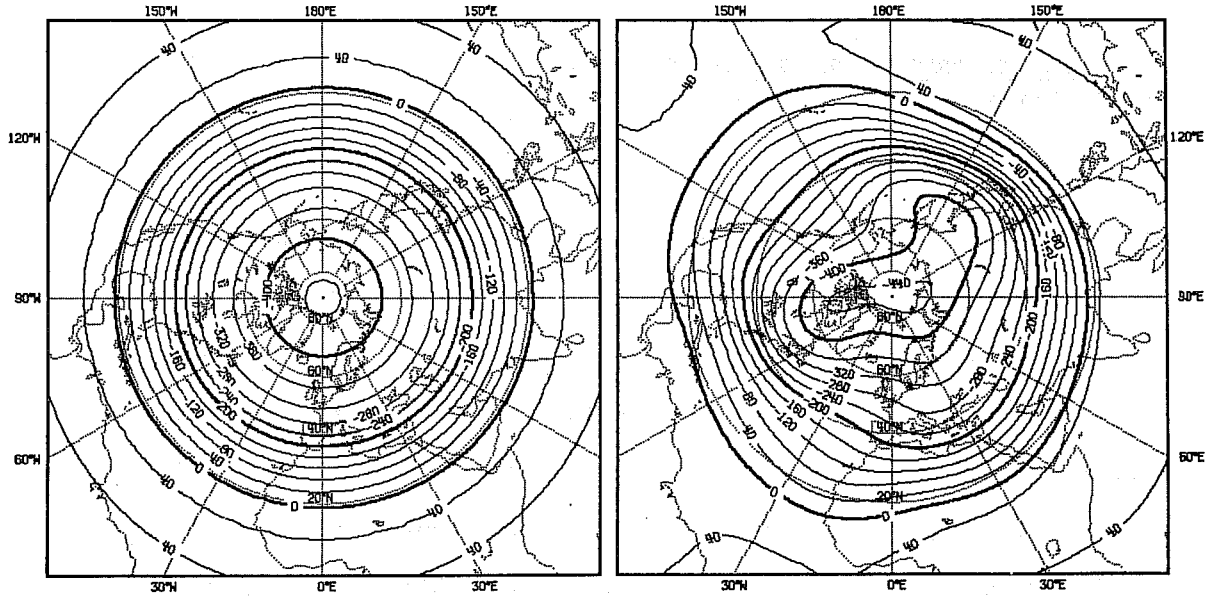

Fig. 15 Zonal-mean (left) and total (right) 300 mb stream functions for the January climatology.

The isolated forcing is specified by a term - fD, where f is the Coriolis parameter. The 'divergence' D has the spatial distribution given by the zonally non-uniform part of Eqn. (9) and a maximum value of 2×10^{-6} s^{-1}. This is half the maximum value used by Hoskins and Karoly (1981) and, as noted by these authors, it corresponds approximately to the value associated with a tropical rainfall maximum of 5 mm/day.

7.2 Zonally uniform basic flows

Perturbation fields at days 5 and 10 are shown in Fig. 16 for a forcing centred at 15°N, 135°E and the 300 mb January zonal-mean flow. In agreement with a similar calculation presented by Hoskins and Karoly the forcing excites a train of waves which by day 10 bears a clear similarity to results obtained using the steady primitive equation model. Results in Fig. 16 are presented not only for the stream function but also for the corresponding geopotential obtained from the linear balance equation. In subsequent plots of the stream function it should be borne in mind that the contour value corresponds approximately to a 4 dam contour interval in height in polar regions. It should also be noted that although non linear calculations are presented, amplitudes are, except where stated, sufficiently small for non linear effects to be weak. The response to a larger forcing may thus be deduced simply by an appropriate increase in the amplitude of the solution illustrated.

The sensitivity of the response to the latitude of maximum forcing is illustrated in Fig. 17, again for the zonal mean basic state. Although the solutions for forcing maxima at 5°N and 5°S exhibit smaller amplitudes than for forcing maximum at 15°N, as found previously, the Northern Hemisphere response at day 10 to a forcing centred at 15°S is larger than suggested by the earlier steady calculation. A similar enhancement of cross-equatorial propagation due to transient effects has been noted in the case of

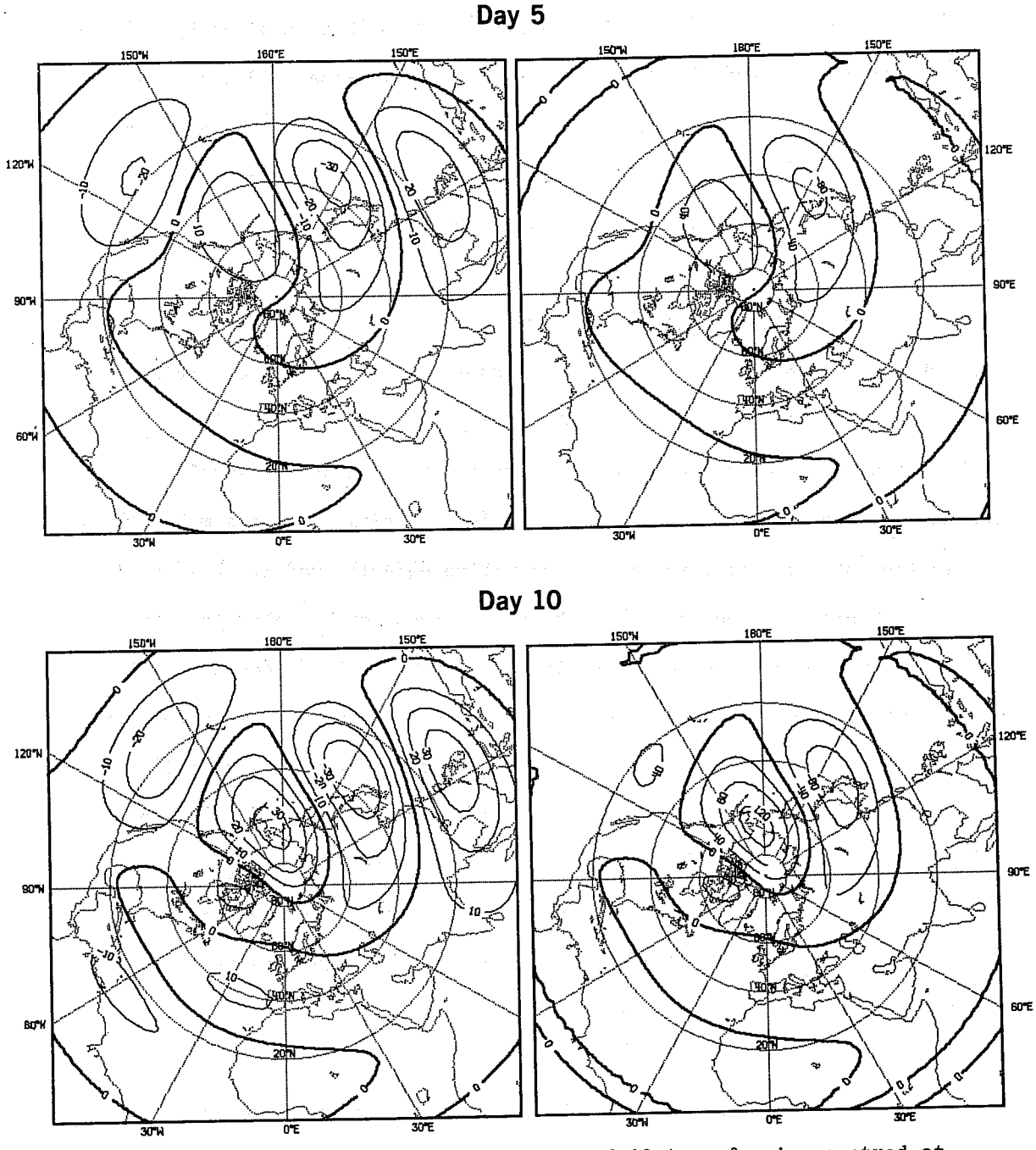

Fig. 16 The barotropic response at days 5 and 10 to a forcing centred at 15^{o}N, 135^{o}E. The stream function (left) is non-dimensionalized by a factor $10^{-4}a^{2}\Omega$. The contour interval for the height field (right) is 4 dam.

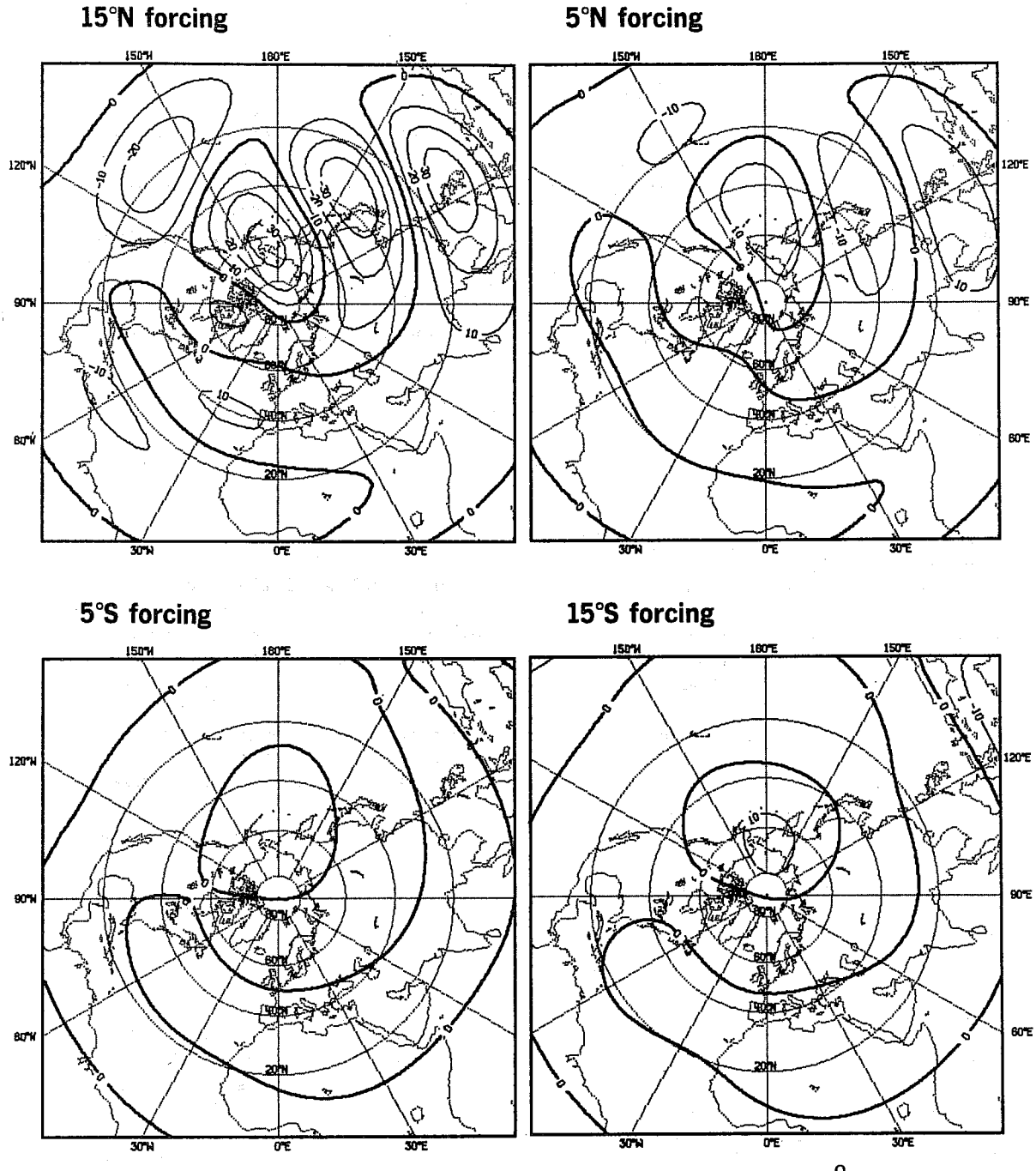

Fig. 17 The stream-function response to forcings centred at 135°E and various latitudes for a zonally-uniform flow.

mid-latitude forcing by Hoskins et al (1977).

An enhanced cross-equatorial propagation associated with temporal variations in the amplitude of a stationary forcing may be illustrated by considering the example of the long-term response to a stationary forcing whose amplitude varies sinusoidally in time. This forcing may be resolved into a sum of steady eastward and westward moving components. If the frequency of the forcing is sufficiently high the westward component will be associated with no critical latitude, and a significant cross equatorial propagation may occur.

7.3 Zonally non-uniform basic flows

Fig. 18 illustrates one of the most interesting results of this study, namely that a particularly large response can be found in the case of a zonally-varying basic flow. This figure compares solutions at days 5 and 10 for the zonal mean and zonally varying January climatological basic flow. Although the solution in the latter case is generally larger than in the former, the most striking feature is the isolated region of anomalously large amplitude located in the region of the climatological ridge in the North East Pacific.

The result shown in Fig. 18 for forcing centred at 135°E is atypical in that forcings at other longitudes do not excite as large a response, but Fig. 19 shows that for forcings centred at three other longitudes 90° apart the maximum amplitude occurs close to the same region of the Pacific. The forcing centred at 80°W, for which results are also shown in Fig. 19, lies south of the North American jet maximum, and in this case the largest response occurs over the Atlantic to the west of Europe, although it is still not as large as in the corresponding Pacific case shown in Fig. 18. Generally similar results are found for forcings centred at 15°N although, as in earlier examples, amplitudes are generally larger than found for the 5°N forcings.

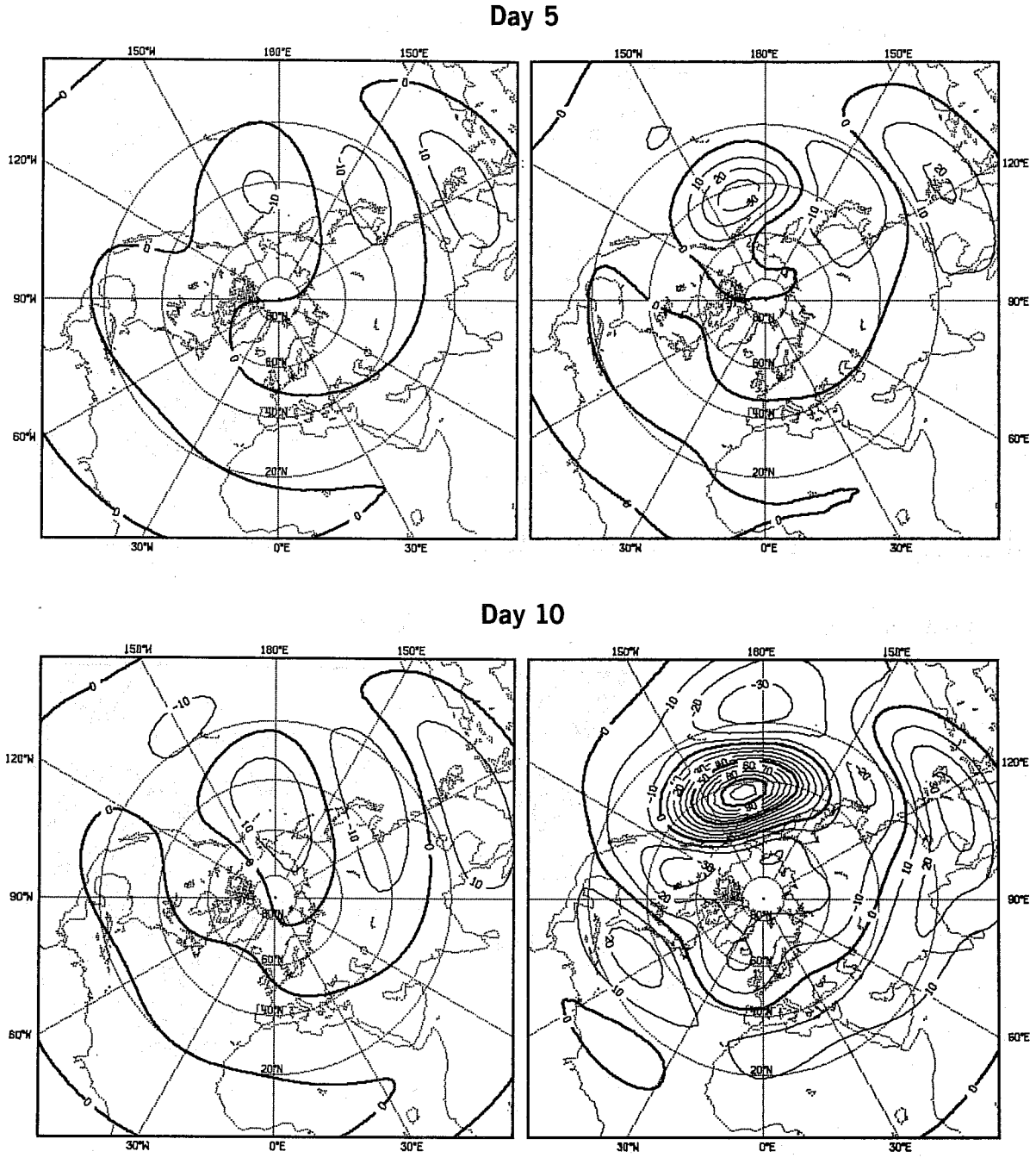

Fig. 18 The response at days 5 and 10 to a forcing centred at 5°N, 135°E for a zonally-uniform climatological basic flow (left) and for the corresponding zonally-varying flow (right).

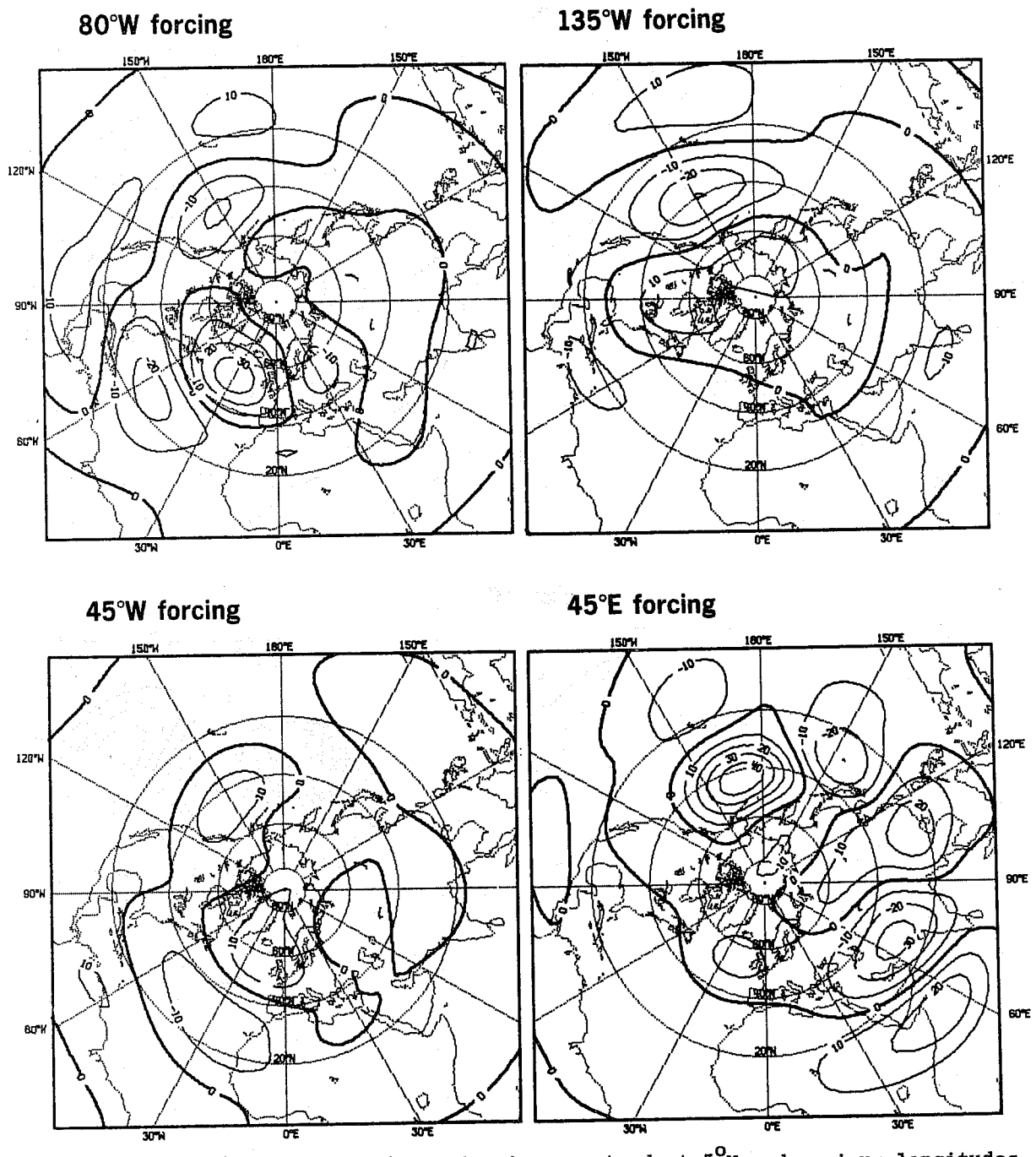

Fig. 19 The response at day 10 to forcings centred at 5°N and various longitudes for the zonally-varying basic flow.

7.4 The mechanism of the large-amplitude response

The mechanism whereby a large amplitude disturbance develops in the North East Pacific region can be seen by examination of the vorticity budget. We write the absolute vorticity, ζ, and the velocity components, u and v, as sums of basic flow (climatological mean) values, ζ_m, u_m, v_m, and perturbation values ζ', u', v'. For small perturbation amplitudes the tendency of ζ' is given (outside the forcing region and neglecting dissipation) by

$$\frac{\partial \zeta'}{\partial t} = - \frac{u_m}{a\cos\theta} \frac{\partial \zeta'}{\partial \lambda} - \frac{v'}{a} \frac{\partial \zeta_m}{\partial \theta} - \frac{u'}{a\cos\theta} \frac{\partial \zeta_m}{\partial \lambda} - \frac{v_m}{a} \frac{\partial \zeta'}{\partial \theta} \qquad (11)$$

The last two terms on the right-hand side are zero in the case of a zonally-uniform basic flow. The first two terms represent, respectively, the advection of perturbation vorticity by the basic zonal flow, and the advection of the absolute vorticity associated with the basic state by the perturbation meridional velocity.

The terms in (11) have been evaluated at day 5 for the cases shown in Fig. 18. A high degree of cancellation makes the interpretation of contour maps difficult to present, and results are thus illustrated for just one latitude, close to 40°N. Here the vorticity tendency is dominated for the non-uniform basic flow by the first two terms on the right-hand side of (11), and these terms are shown in the upper plot of Fig. 20, together with the net tendency due to all four terms. Corresponding plots (on a different scale) for the zonally-uniform basic flow are also shown. For the non-uniform case the magnitudes of the last two terms on the right-hand side are individually of the order of the residual of the first two terms, but these last two terms also largely cancel.

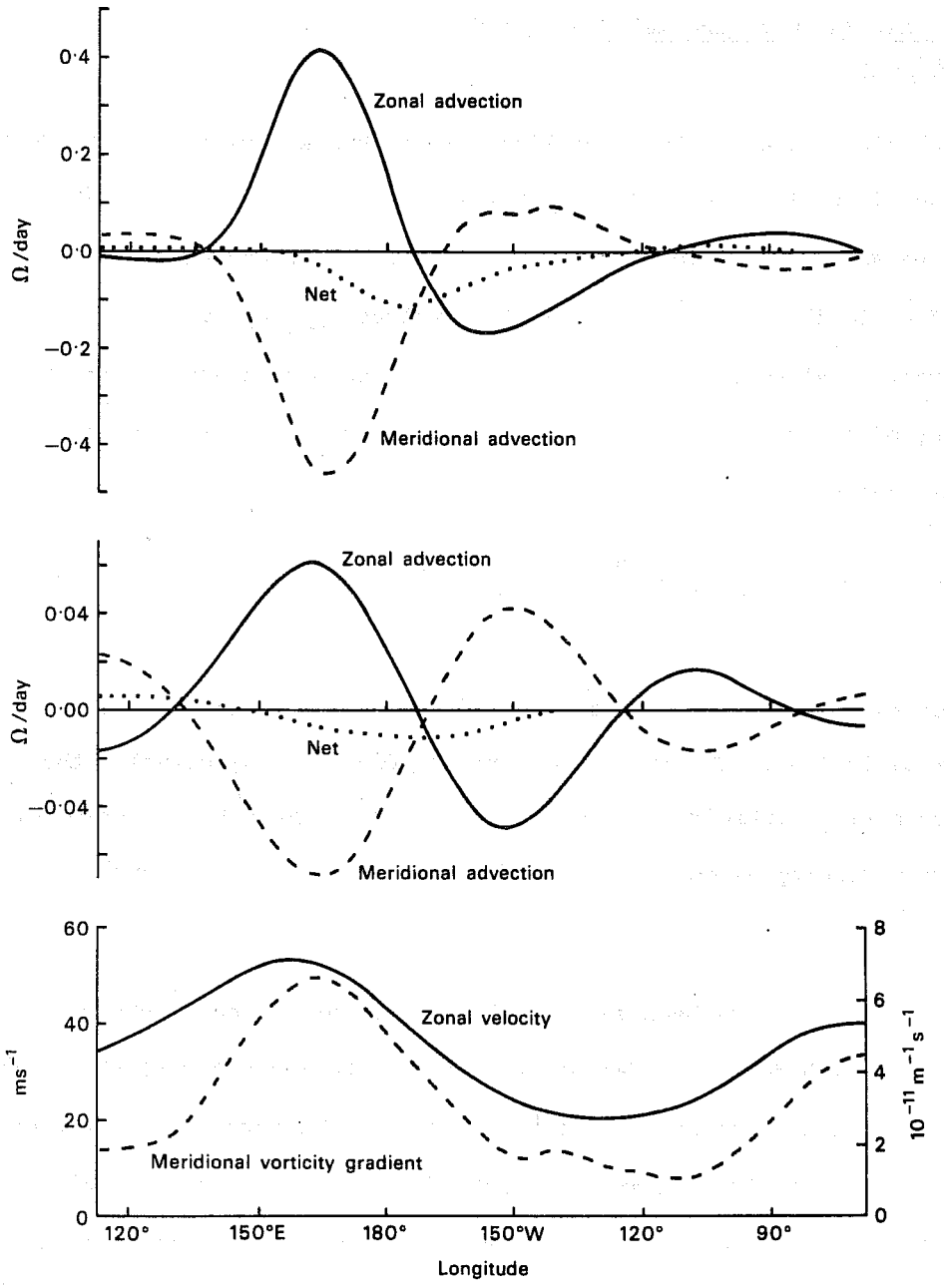

Fig. 20 The variation with longitude at latitude 39.4°N of various terms of relevance to the vorticity budget for the cases shown at day 5 in Fig. 18. The upper two plots show the net vorticity tendency (dotted) for the zonally-varying basic flow (upper) and for the zonal-mean basic flow, plus the contributions to this tendency from the advection of perturbation vorticity by the zonal component of the basic flow (solid lines) and from the advection of the absolute vorticity of the basic state by the perturbation meridional velocity (dashed lines). The bottom plot shows the basic zonal velocity and the meridional gradient of absolute vorticity of the basic state for the non-uniform case. Corresponding zonal mean values are 29 ms^{-1} and 2.2 x 10^{-11} $m^{-1}s^{-1}$.

Fig. 20 shows that the net negative vorticity tendency, which is such as to reinforce the local anticyclonic maximum near 160°W, arises as a result of advection of basic vorticity by the perturbation being slightly the larger upstream of the disturbance maximum and advection of perturbation vorticity by the basic zonal flow being slightly the larger downstream of the maximum. The imbalance between the two terms is relatively larger for the non-uniform basic flow, and may be directly related to the longitudinal variations of the basic flow and poleward vorticity gradient, which are illustrated in the lower part of Fig. 20. The vorticity gradient is

$$\frac{1}{a}\frac{\partial \zeta_m}{\partial \theta} = \frac{2\Omega\cos\theta}{a} - \frac{1}{a^2}\frac{\partial}{\partial \theta}\left[\frac{1}{\cos\theta}\left(\frac{\partial v_m}{\partial \lambda} - \frac{\partial}{\partial \theta}(u_m\cos\theta)\right)\right]$$

and as the basic flow is non divergent this may be approximated in middle latitudes by

$$\frac{2\Omega\cos\theta}{a} - \nabla^2 u_m$$

if mean flow variations occur on a length scale smaller than the radius of the earth. The gradient thus depends both on the strength of the basic zonal flow and on the length scale of its meridional and zonal variation, and in the region of maximum anticyclonic disturbance (from 160°E to 120°W) it varies proportionally more with longitude than does the basic zonal flow. This, coupled with the large values of the basic zonal flow and vorticity gradient upstream of the disturbance maximum, leads to the larger imbalance in the dominant terms on the right-hand side of (11). Thus, while at day 5 the amplitude of the disturbance in the case of the non-uniform basic state is about three times larger than that for the zonal-mean basic state, the vorticity tendency is about ten times larger in the region of largest disturbance.

A generally similar picture holds at other latitudes near or to the south of the latitude of maximum disturbance. To the north east a region of negative $\overline{\zeta_\theta}$ occurs for the non-uniform basic state, and this gives a region of positive vorticity tendency which cannot be balanced by advection by the locally weak basic zonal flow. Here, however, this component of the tendency is more than compensated by a large contribution from the fourth term in (11), that is by a significant advection of the negative perturbation vorticity by the locally large northward component of the basic flow.

The relatively large amplitudes found when the forcing is located equatorward of regions of particularly strong basic flow may be accounted for by examination of the initial vorticity budget. Consider, for simplicity, a zonally-uniform basic state with zonal velocity $\bar{u}$ and a forcing F. The linearized perturbation vorticity equation is then

$$\frac{\partial \zeta'}{\partial t} = - \frac{\bar{u}}{a\cos\theta} \frac{\partial \zeta'}{\partial \lambda} - \frac{\beta_* v'}{\cos^2 \theta} + F \quad , \tag{12}$$

where β_* is given by (7).

A characteristic of a strong westerly jet-like flow is the presence of regions of relatively small $\bar{u}$ and β_* near the equatorward and poleward limits of the jet. In such regions any local forcing F must initially be balanced by the tendency $\partial\zeta'/\partial t$, implying a relatively large local growth of the perturbation vorticity. Associated with this vorticity will be a meridional velocity field, v', of larger meridional scale than the vorticity, and this velocity may generate perturbation vorticity in the vicinity of the jet maximum through the second term on the right-hand side of (12). The stronger and narrower the jet, the larger will be β_*, and the larger will be this generation of perturbation vorticity. As time

progresses this vorticity may disperse, a dispersion facilitated by larger values of β_*, to give a large response more distant from the region of forcing.

7.5 The non-linear response

The particularly large amplitude solutions found for forcing centred at 15°N, 135°E may be used to illustrate the role of nonlinearity in modifying the response. Fig. 21 compares linear and non-linear solutions for this case with those for the case in which the sign of the forcing is reversed. In the former case, shown on the left-hand side of Fig. 21, anticyclonic vorticity develops in the region of large response, and non linearity marginally increases the amplitude of the response. In the latter case the linear solution is simply opposite in sign to that obtained in the former case, but the non linear solution shows the amplitude of the response to be substantially reduced.

The role of non linearity may be easily understood. In the former case the anticyclonic response in the North East Pacific reinforces the climatological ridge, which has been shown to be responsible for the anomalous response in the first place. A positive feedback occurs, giving the strong ridge shown in the maps of total streamfunction presented in Fig. 22. Conversely, for cyclonic forcing the cyclonic response tends to reduce the climatological ridge, and thus damp itself.

7.6 Cross-equatorial propagation

Another important effect of introducing a zonally-varying basic flow is a marked influence on the degree of cross-equatorial propagation. For the zonal mean climatology, winds are easterly at the equator. The Northern Hemisphere response to a forcing at 15°S has been shown for day 10 in Fig. 17, and beyond this time its amplitude weakens to give the particularly small long-term response indicated by the steady-state calculations.

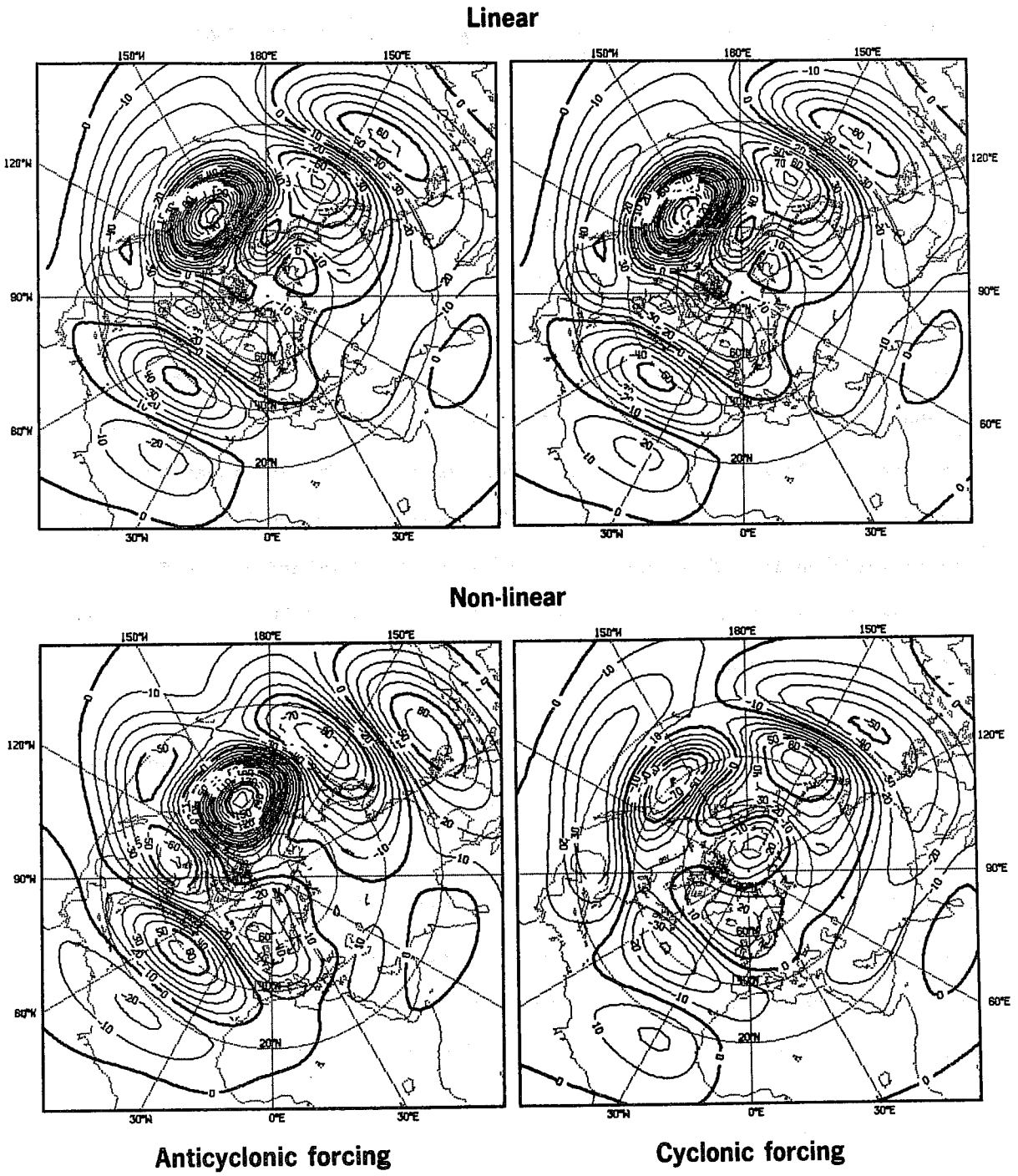

Fig. 21 A comparison of linear (upper) and non-linear (lower) responses to anticyclonic (left) and cyclonic (right) forcing.

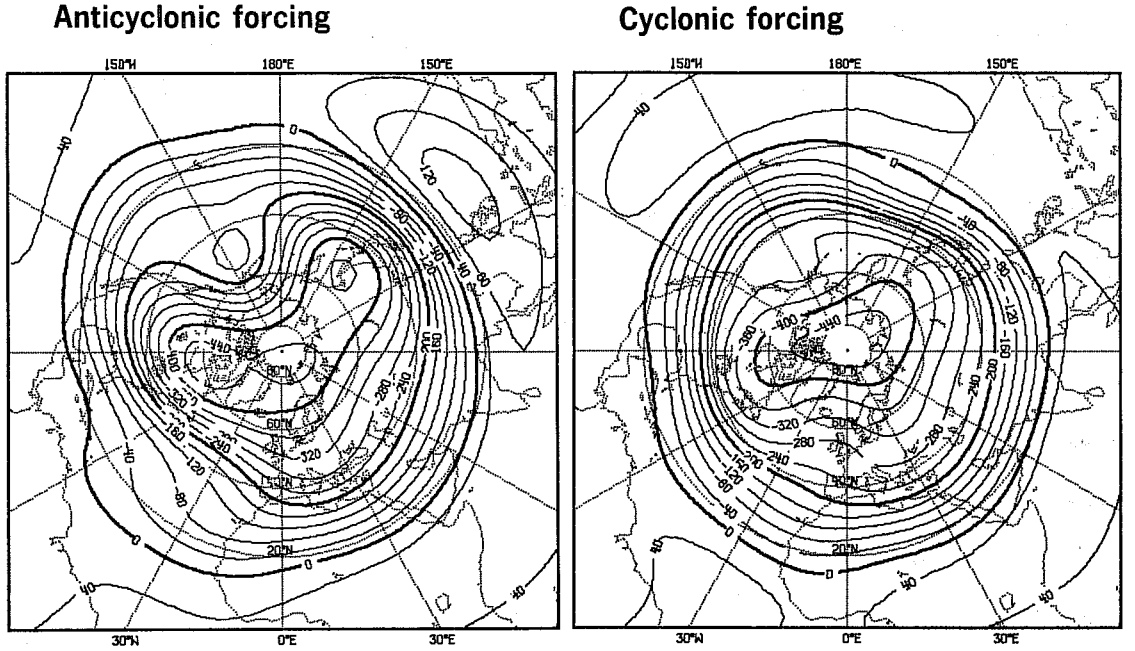

Fig. 22 The total stream function corresponding to the perturbation fields shown in the lower half of Fig. 21.

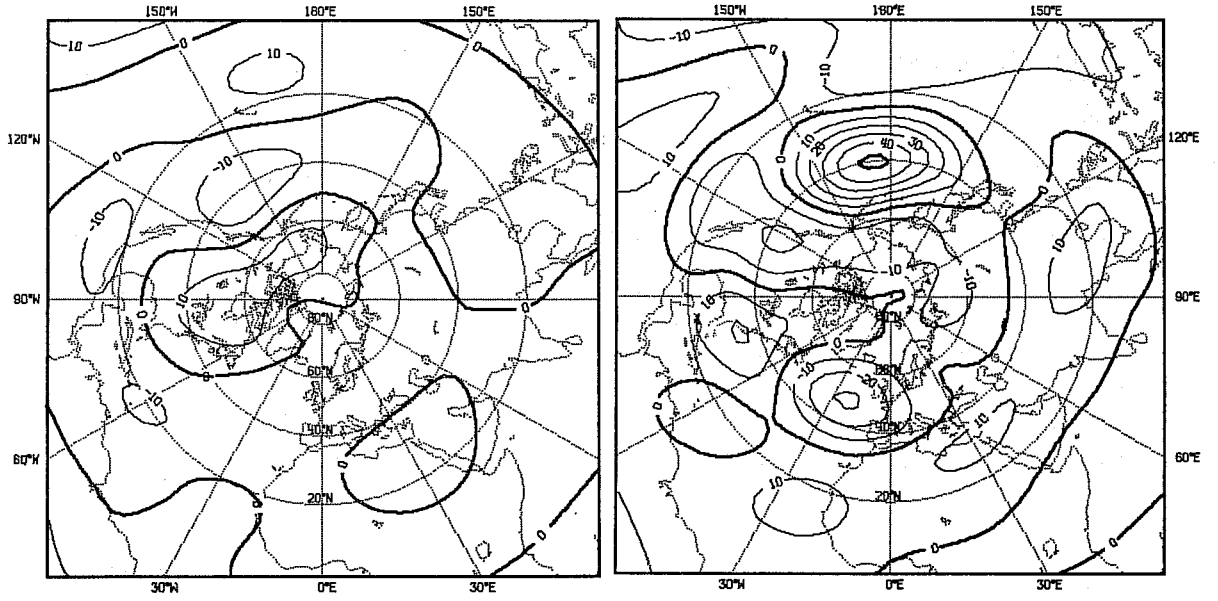

Fig. 23 The Northern Hemisphere response at days 10 (left) and 30 (right) for a forcing centred at 15°S, 135°W for the zonally-varying basic flow.

A quite different result is shown in Fig. 23 for the zonally-varying January flow and a forcing at 15°S, 135°W. At day 10 the maximum amplitude of the Northern Hemisphere response differs little from that in the case of the zonal-mean flow, but beyond this time the amplitude increases, rather than decays. Thus, by day 30 a much larger wave amplitude is found, particularly in the North Pacific region which we have already seen to be a favourable region for a large-amplitude response.

This result confirms a speculation by Webster (1981) that cross-equatorial propagation may occur through regions of westerly flow of limited longitudinal extent, such as appear in seasonal means. Such westerly flow occurs over the East Pacific for the 300 mb level used for the calculations shown in Fig. 23. Repetition of these calculations for a basic flow modified between 20°N and 20°S in order to remove the region of westerly equatorial wind showed a substantial drop in the Northern Hemisphere response.

7.7 Other calculations

A number of other calculations have been performed. No significant differences result from a more gradual initiation of the forcing. A relatively large North Pacific response to a forcing from the Northern Hemisphere tropics is found for the January 500 mb flow, although this is weaker than found for the 300 mb flow. The 500 mb flow is easterly at all equatorial longitudes, and no significant cross-equatorial propagation is found. The standing wave pattern in the Northern Hemisphere is substantially weaker in the July climatology, and no significant modification of the response obtained for a zonal-mean flow has been found in this case.

8. A FORECAST EXPERIMENT INVOLVING RELAXATION TOWARDS ANALYSED TROPICAL FIELDS

As a final topic we present results from the first forecast experiment in a series intended to quantify our knowledge of the influence of the tropics on middle latitudes in the context of medium range prediction. Details of the experiment have already been discussed in Sect. 3c.

The impact of relaxing the forecasts towards analyzed values equatorward of 30° latitude is summarized by the objective verification presented in Fig. 24. Although the standard area chosen for verification includes part of the forcing region, the contribution from the latter is small, and most of the differences shown in Fig. 24 arise due to changes in the forecast fields in middle and high latitudes.

The standard forcast for this case from June 1979 was characterized in the tropics by a poor forecast of the onset of the South West Monsoon. Despite this, the impact of relaxing towards tropical analyses is shown both by Fig. 24 and by examination of synoptic maps to be small in the Northern Hemisphere. This is in broad agreement with the results from the simpler models discussed earlier, which show little extratropical response to steady tropical forcing for the Northern Hemisphere summer.

A more substantial impact is evident in the Southern (winter) Hemisphere. This is only partly shown in the objective scoring of the total field because of a poor forecast of the medium scales of motion in both cases. For the longer waves, however, Fig. 24 shows a substantial improvement to result from the tropical relaxation, which prevents the sudden fall in anomaly correlation which occurs beyond day 6 in the standard forecast. This is also evident in the 500 mb height maps presented in Fig. 25 for the day 8 forecast. These show a clear improvement as far south as the 60° - 80° latitude band.

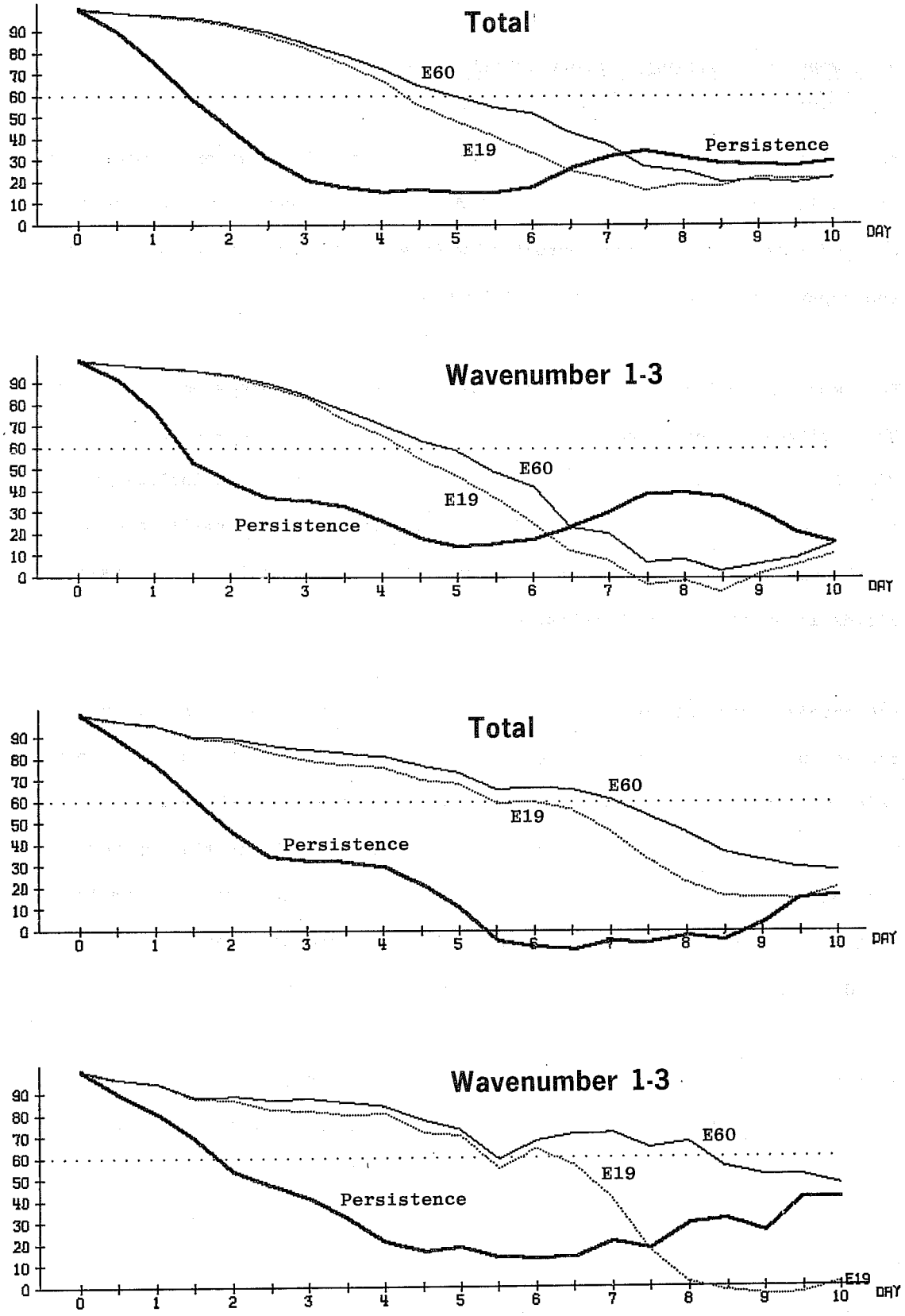

Fig. 24 Anomaly correlations of the height field averaged from 1000 to 200 mb and from 20°-82.5°N (upper) and 20°-82.5°S (lower). E19 denotes the standard experiment and E60 the experiment with tropical relaxation.

Analysis

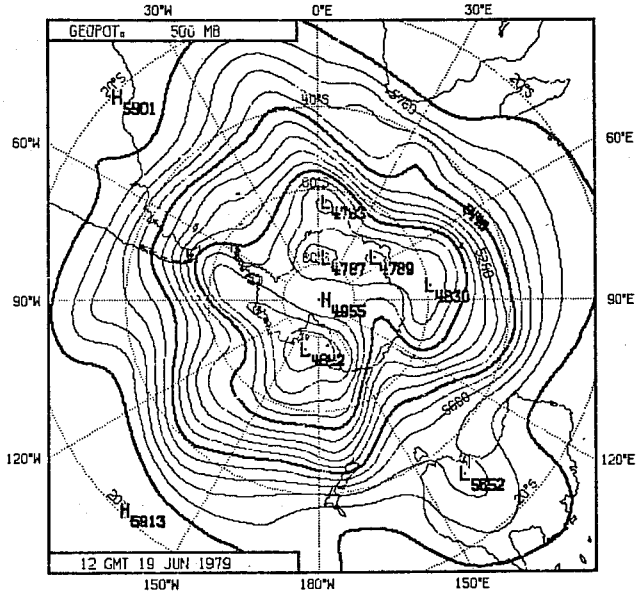

Forecast with tropical relaxation

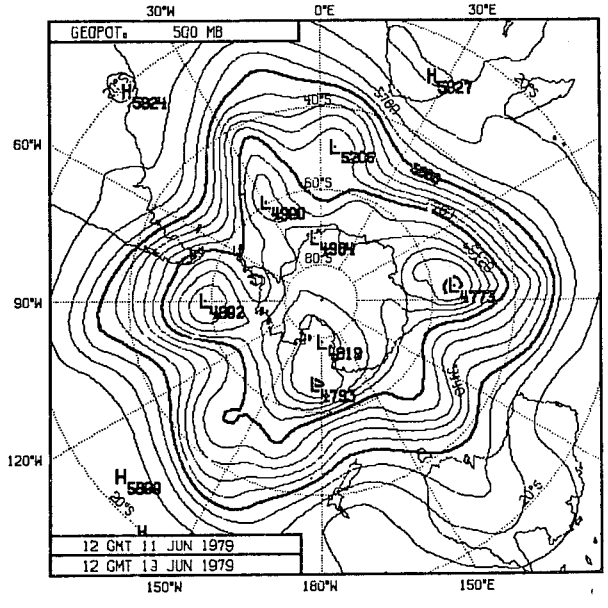

Control forecast

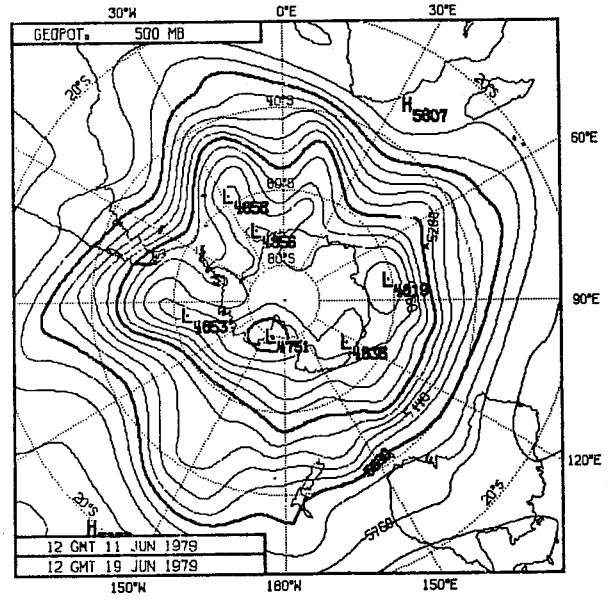

Fig. 25 Maps of the 500 mb height field for day 8. The contour interval is 8 dam.

Although Northern Hemisphere maps do not illustrate as marked a sensitivity to the tropical representation, the difference maps presented in Fig. 26 give a picture of the rate at which differences spread from particular regions of the subtropics, and grow. These differences can be related to differences in the amplitude and phase of clearly identifiable features which exist in both forecasts, and the spatial scale of the differences spread latitudinally at a rate similar to that of their zonal spreading.

9. CONCLUDING REMARKS

It is difficult to assess quantitative aspects of the simple model results presented here for a number of reasons, in particular because of the presence in reality of significant interactions between standing and transient waves and perhaps also because of the lack of any direct vorticity forcing or dissipation to accompany the imposed diabatic heating which was chosen to model the effect of an area of tropical convection. However, if results of studies such as this are combined with those of observational and general circulation model studies a coherent picture is obtained which shows a marked influence of the tropics on the standing wave pattern in the middle and high latitudes of at least the winter hemisphere. This is borne out to some extent by the single forecast experiment also reported here, but caution must of course be exercised in drawing conclusions from just one such experiment.

From the idealized model studies it may be seen that it is important to simulate accurately the geographical distribution, the magnitude, and the temporal variability of the tropical convective heating in order to represent accurately its effect on stationary motion in middle latitudes. A particularly accurate vertical profile of heating does not appear to be as important in this respect. It is also important to represent the detailed structure of the mid-latitude jet in order to obtain the correct

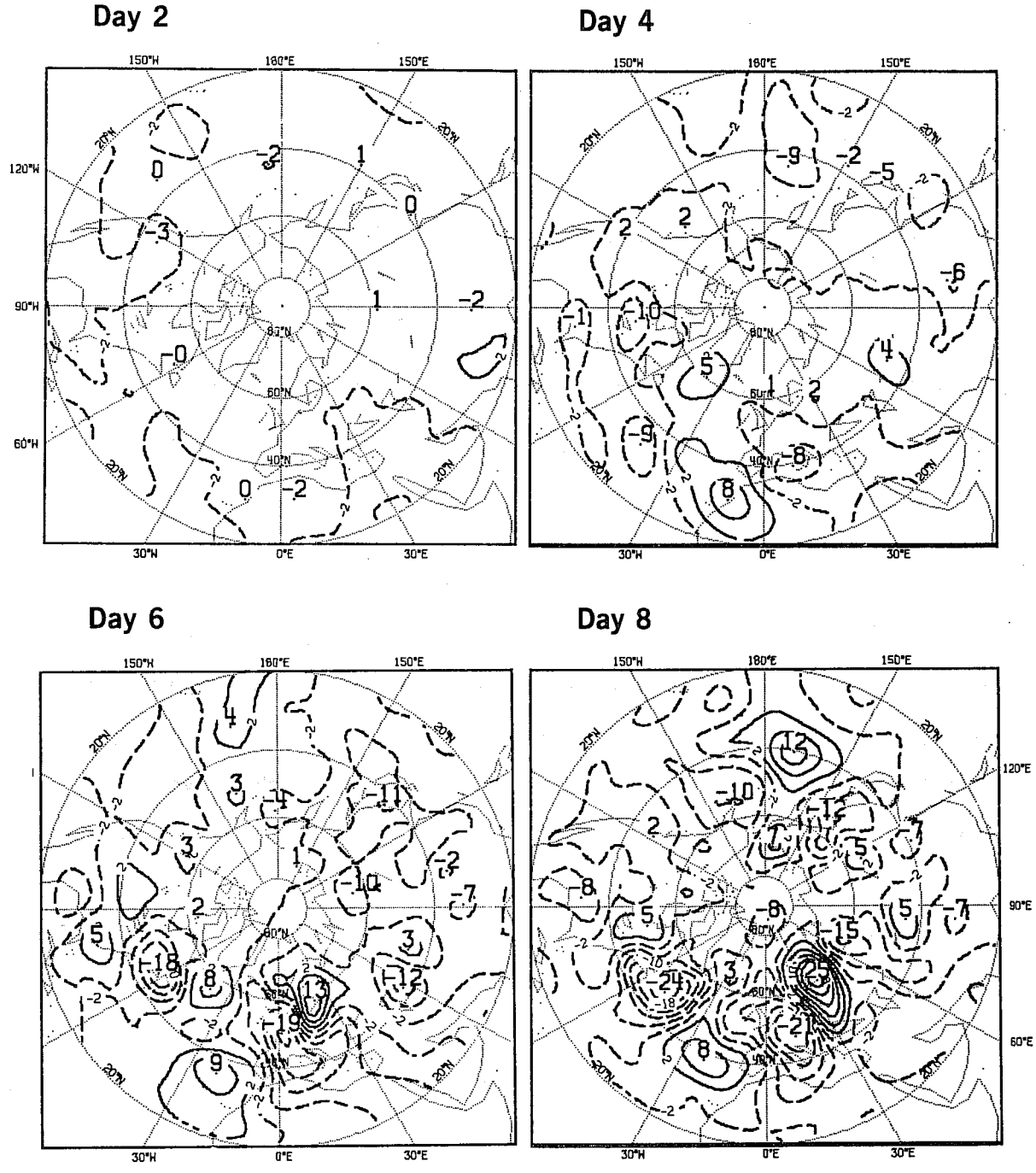

Fig. 26 The difference between the 500 mb heights of the control forecast and the forecast with tropical relaxation for day 2 (upper left), day 4 (upper right), day 6 (lower left) and day 8 (lower right). The contour interval is 4 dam.

response to tropical forcing.

The barotropic solutions for a zonally-varying basic flow show that in favourable circumstances there can be a significant interaction between a pre-existing forced stationary wave and wave motion forced from an isolated tropical region. This raises the possibility that experiments with a general circulation model may substantially underestimate the effect of anomalous boundary conditions, for example sea surface temperature anomalies, if the model used underestimates the climatological standing wave pattern. A second result of these calculations is that substantial cross-equatorial propagation may occur in the presence of an equatorial region of westerly flow of limited longitudinal extent.

A possible deficiency of these barotropic calculations is that the zonally-varying basic flow is maintained by a constant forcing rather than by one which changes with the motion as the additional tropical forcing is introduced. Further study of the large response found in this case is evidently required.

Acknowledgements

The steady-state and forecast experiments involving relaxation were suggested by D.M. Burridge. The forecast experiments were carried out by J.M. Haseler. Helpful comments on the text of this report have been made by A. Hollingsworth and B.J. Hoskins.

REFERENCES

Bjerknes, J. 1966 A possible response of the atmospheric Hadley circulation to equatorial anomalies of ocean temperature. Tellus, 18, 820-829.

Bjerknes, J. 1969 Atmospheric teleconnections from the equatorial Pacific. Mon.Wea.Rev., 97, 163-172.

Burridge, D.M. and J.M. Haseler 1977 A model for medium range weather forecasting - Adiabatic formulation. ECMWF Tech.Rep. No.4, 46 pp.

Charney, J.G. 1969 A further note on large-scale motions in the Tropics. J.Atm.Sci., 20, 607-609.

Charney, J.G. and Drazin 1961 Propagation of planetary-scale disturbances from the lower into the upper atmosphere. J.Geophys.Res, 74, 83-109.

Dunkerton, T.J., C.-P. Hsu and M.E. McIntyre 1981 Some Eulerian and Lagrangian diagnostics for a model stratospheric warming. To appear in J.Atmos.Sci.

Egger, J. 1977 On the linear theory of the atmospheric response to sea surface temperature anomalies. J.Atmos.Sci., 34, 603-614.

Geisler, J.E. and R.E.Dickinson 1974 Numerical study of an interacting Rossby wave and barotropic zonal flow near a critical level. J.Atmos.Sci., 31, 946-955.

Grose, W.L. and B.J. Hoskins 1979 On the influence of orography on large-scale atmospheric flow. J.Atmos.Sci., 36, 223-234.

Hollingsworth, A., K. Arpe, M. Tiedtke, M. Capaldo, H.Savijärvi, O.Åkesson, J.A. Woods 1980 Comparison of Medium Range Forecasts made with two parameterization schemes. ECMWF Tech. Rep. No.13, 214pp.

Holton, J.R. 1979 An introduction to dynamical meteorology. 2nd Ed., Academic Press, 391pp.

Horel, J.D. and J.M. Wallace 1981 Planetary scale atmospheric phenomena associated with the interannual variability of sea-surface temperature in the equatorial Pacific. Submitted to Mon.Wea.Rev.

Hoskins, B.J. and A.J. Simmons 1975 A multi-layer spectral model and the semi-implicit method. Quart.J.Roy.Met.Soc., 101, 637-655.

Hoskins, B.J., A.J. Simmons and D.G. Andrews 1977 Energy dispersion in a barotropic atmosphere. Quart.J.Roy.Met.Soc., 103, 553-567.

Hoskins, B.J. and D.J. Karoly 1981 The steady linear response of a spherical atmosphere to thermal and orographic forcing. Submitted to J.Atmos.Sci.

Julian, P.R. and R.M. Chervin 1978 A study of the southern oscillation and Walker circulation phenomena. Mon.Wea.Rev., 106, 1433-1451.

Lau, N.C. 1979 The observed structure of tropospheric stationary waves and the local balance of vorticity and heat. J.Atmos.Sci., 36, 996-1016.

Lau, N.C. and J.M. Wallace 1979 On the distribution of horizontal transports by transient eddies in the Northern Hemisphere wintertime circulation. J.Atmos.Sci., 36, 1844-1861.

Lindzen, R.S. and H.L. Kuo 1969 A reliable method for the numerical integration of a large class of ordinary and partial differential equations. Mon.Wea.Rev., 96, 732-734.

Lindzen, R.S. and K.K. Tung 1978 Wave overreflection and shear instability. J.Atmos.Sci., 35, 1626-1632.

Opsteegh, J.D. and H.M. van den Dool 1980 Seasonal differences in the stationary response of a linearised primitive equation model: prospects for long range weather forecasting? J.Atmos.Sci., 37, 2169-2185.

Rowntree, P.R. 1972 The influence of tropical east Pacific Ocean temperatures on the atmosphere. Quart.J.Roy.Met.Soc.,98, 290-321.

Rowntree, P.R. 1976 Response of the atmosphere to a tropical Atlantic ocean temperature anomaly. Quart.J.Roy.Met.Soc., 102, 607-626.

Simmons, A.J. 1978 Some effects of meridional shear and spherical geometry on long stratospheric waves. Quart.J.Roy.Met.Soc., 104, 595-614.

Stewartson, K. 1978 The evolution of the critical layer of a Rossby wave. Geophys.Astrophys.Fluid Dyn., 9, 185-200.

Tiedtke, M. J.-F. Gelyn, A. Hollingsworth, J.-F. Louis 1979 ECMWF Model-Parameterization of sub-grid scale processes. ECMWF Tech.Rep. No.10, 46pp.

Tung, K.K. 1979 A theory of stationary long waves. Part III: Quasi-normal modes in a singular waveguide. Mon.Wea.Rev., 107, 751-774.

Tung, K.K. and R.S. Lindzen 1979 A theory of stationary long waves. Part I: A simple theory of blocking. Mon.Wea.Rev., 107, 714-734.

Wallace, J.K. and D.S. Gutzler 1981 Teleconnections in the geopotential height field during the Northern Hemisphere winter. Mon.Wea.Rev., 109.

Webster, P.J. 1981 Mechanisms determining the atmospheric response to sea surface temperature anomalies. J.Atmos.Sci., 38, 554-571.

APPENDIX

THE LINEAR, STEADY-STATE MODEL

The linearized primitive equations, including a diabatic heating $c_p Q$, Newtonian cooling with rate δ, and Rayleigh friction with rate ε, may be written

$$\frac{1}{a(1-\mu^2)}\ \bar{U}\frac{\partial U'}{\partial\lambda} + V'\ (-2\Omega\mu + \frac{1}{a}\frac{\partial\bar{U}}{\partial\mu}) + \dot{\sigma}\frac{\partial\bar{U}}{\partial\sigma} + \frac{1}{a}\frac{\partial\phi'}{\partial\lambda} + \frac{R\bar{T}}{a}\frac{\partial\ell np_s}{\partial\lambda} = -\varepsilon U' \qquad (A.1)$$

$$\frac{1}{a(1-\mu^2)}\ \bar{U}\frac{\partial V'}{\partial\lambda} + 2\Omega\mu\ U' + \frac{2\mu}{a(1-\mu^2)}\ \bar{U}U' + \frac{1}{a}\ (1-\mu^2)\ \frac{\partial\phi'}{\partial\mu} + \frac{R}{a}(1-\mu^2)\{\bar{T}\frac{\partial\ell np_s'}{\partial\mu} + T'\frac{\partial\overline{\ell np_s}}{\partial\mu}\} = -\varepsilon V' \qquad (A.2)$$

$$\frac{1}{a(1-\mu^2)}\ \bar{U}\frac{\partial T'}{\partial\lambda} + V'\frac{1}{a}\frac{\partial\bar{T}}{\partial\mu} + \dot{\sigma}\frac{\partial\bar{T}}{\partial\sigma} - \frac{\kappa\bar{T}\omega}{p} = -\delta T' + Q \qquad (A.3)$$

$$\frac{1}{a}\int_0^1 \{\frac{1}{(1-\mu^2)}\ \bar{U}\frac{\partial}{\partial\lambda}\ell np_s' + V'\frac{\partial}{\partial\mu}\overline{\ell np_s} + \frac{1}{(1-\mu^2)}\frac{\partial U'}{\partial\lambda} + \frac{\partial V'}{\partial\mu}\}\ d\sigma = 0 \qquad (A.4)$$

where U and V are the eastward and northward velocity components multiplied by the cosine of latitude and μ is the sine of latitude. An overbar denotes a zonal-mean field, and a prime denotes a deviation from the zonal mean. Other symbols have their usual meaning.

We solve separately for each zonal wavenumber component of the perturbation, using a grid staggered in the north-south. We let U^n, T^n and ℓ^n denote the complex amplitudes of U', T' and $\ell np_s'$ at latitude $\pi/2 - n\Delta\theta$ written as column vectors with elements corresponding to each of the NLEV model levels. iV^n denotes the corresponding complex amplitudes of the V' at latitude $\pi/2-(n+\frac{1}{2})\Delta\theta$. Here $\Delta\theta = \pi/N$, with N the number of grid lengths from pole to pole. Introducing second-order accurate finite-difference approximations, (A.1) to (A.4) may be written in the form

$$M_1^nU^n + M_2^nV^n + M_3^nT^n + N_1^n\ell^n - i\varepsilon IU^n + M_2^{n-}V^{n-1} = -m\phi_s^n \qquad (A.5)$$

$$M_4^nU^n + M_5^nV^n + M_6^nT^n + N_2^n\ell^n + i\varepsilon IV^n + M_4^{n+}U^{n+1} + M_6^{n+}V^{n+1} + N_2^{n+}\ell^{n+1} = -R_1^n\phi_s^n - R_1^{n+}\phi_s^{n+1}$$

$$M_7^nU^n + M_8^nV^n + M_9^nT^n + N_3^n\ell^n - i\delta IT^n + M_8^{n-}V^{n-1} = -iQ^n \qquad (A.7)$$

$$P_1^nU^n + P_2^nV^n + R_2^n\ell^n + P_2^{n-}V^{n-1} = 0 \qquad (A.8)$$

Here M_i^n, M_i^{n+}, and M_i^{n-} are real matrices of dimension NLEVxNLEV with values at each latitude n, N_i^n and N_2^{n+} are real column vectors, P_i^n and P_2^{n-} are real row vectors, and R_i^n and R_1^{n+} are real scalars. ϕ_s^n is the complex amplitude of the surface value of the geopotential at latitude n which, together with the corresponding diabatic term Q^n forces the wave motion. I is the unit matrix.

The expressions used for the various matrices, vectors and scalars are lengthy, and will not be repeated here. They were derived directly from the operational ECMWF finite-difference scheme (Burridge and Haseler 1977), and non-dissipative, orographically-forced solutions were checked by direct substitution into an adiabatic version of the ECMWF model. As a by-product of the development of this linear model, an error in the polar finite-difference scheme near the poles was detected by examining a poor polar wavenumber 1 structure in a steady solution.

The solution of (A.5) - (A.8) proceeds by reduction to a single equation for the meridional velocity. (A.5) is used to obtain an expression for T^n in terms of U^n, V^n, V^{n-1} and ℓ^n, and (A.7) then gives U^n in terms of V^n, V^{n-1} and ℓ^n. (A.8) may then be used to write ℓ^n in terms of V^n and V^{n-1}. Susbtituting all these expressions into (A.7) finally yields an equation of the form

$$M^{n+} V^{n+1} + M^n V^n + V^{n-} V^{n-1} = F^n \qquad \text{(A.9)}$$

Here M^{n+}, M^n and M^{n-} are (in general complex) NLEVxNLEV matrices and F^n is a complex column vector dependent on the orographic and diabatic forcing.

The solution of (A.9) uses a method devised by Lindzen and Kuo (1969). A solution

$$V^n = \alpha^n V^{n+1} + \beta^n \qquad \text{(A.10)}$$

is proposed, and substituting into (A.9) gives

$$\alpha^n = - (M^{n-} \alpha^{n-1} + M^n)^{-1} M^{n+} \qquad \text{(A.11)}$$

$$\beta^n = (M^{n-} \alpha^{n-1} + M^n)^{-1} (F^n - M^{n-} \beta^{n-1}) \qquad \text{(A.12)}$$

The polar formulation of the finite-difference scheme gives boundary conditions of the form

$$V^{o} = \alpha^{o} V^{1} + \beta^{o} \tag{A.13}$$

$$V^{N-2} = \alpha V^{N-1} + \beta \tag{A.14}$$

so starting with known α_o and β_o we use (A.11) and (A.12) to obtain α^{N-2} and β^{N-2}. V^{N-1} is then determined by using

$$\alpha^{N-2} V^{N-1} + \beta^{N-2} = \alpha V^{N-1} + \beta,$$

which gives $$V^{N-1} = (\alpha^{N-2} - \alpha)^{-1} (\beta - \beta^{N-2}) \tag{A.15}$$

The other V's are then obtained from (A.10) using stored values of α^n and β^n, and other variables are determined using (A.5), (A.7) and (A.8).

As an alternative forcing of the wave motion we include a relaxation towards a prescribed state U'_r, V'_r, T'_r $(\ell np_s')_r$ over a limited range of latitudes. In this case terms $\chi_r(\mu)(U'_r - U')$, $\chi_r(\mu)(V'_r - V')$, $\chi_r(\mu)\ (T'_r - T')$ and $\chi_r(\mu)\ ((\ell np'_s)_r - \ell np'_s)$ are added to the right hand sides of (A.1) to (A.4) respectively. The solution method is unchanged. Note also that the south polar boundary condition (A.14) may be replaced by the condition $V^M = 0$, this corresponding to a vanishing meridional velocity at latitude $\pi/2 - (M+\frac{1}{2})\Delta\theta$. In this case $V^{M-1} = \beta^{M-1}$ and the other V's may again be determined from (A.10) knowing α^n and β^n for $n < M-1$.

ECMWF PUBLISHED TECHNICAL REPORTS

No. 1 A Case Study of a Ten Day Prediction

No. 2 The Effect of Arithmetic Precisions on some Meteorological Integrations

No. 3 Mixed-Radix Fast Fourier Transforms without Reordering

No. 4 A Model for Medium-Range Weather Forecasting - Adiabatic Formulation

No. 5 A Study of some Parameterizations of Sub-Grid Processes in a Baroclinic Wave in a Two-Dimensional Model

No. 6 The ECMWF Analysis and Data Assimilation Scheme - Analysis of Mass and Wind Fields

No. 7 A Ten Day High Resolution Non-Adiabatic Spectral Integration: A Comparative Study

No. 8 On the Asymptotic Behaviour of Simple Stochastic-Dynamic Systems

No. 9 On Balance Requirements as Initial Conditions

No.10 ECMWF Model - Parameterization of Sub-Grid Processes

No.11 Normal Mode Initialization for a multi-level Gridpoint Model

No.12 Data Assimilation Experiments

No.13 Comparison of Medium Range Forecasts made with two Parameterization Schemes

No.14 On Initial Conditions for Non-Hydrostatic Models

No.15 Adiabatic Formulation and Organization of ECMWF's Spectral Model

No.16 Model Studies of a Developing Boundary Layer over the Ocean

No.17 The Response of a Global Barotropic Model to Forcing by Large-Scale Orography

No.18 Confidence Limits for Verification and Energetics Studies

No.19 A Low Order Barotropic Model on the Sphere with the Orographic and Newtonian Forcing

No.20 A Review of the Normal Mode Initialization Method

No.21 The Adjoint Equation Technique Applied to Meteorological Problems

No.22 The Use of Empirical Methods for Mesoscale Pressure Forecasts

No.23 Comparison of Medium Range Forecasts made with Models using Spectral or Finite Difference Techniques in the Horizontal

No.24 On the Average Errors of an Ensemble of Forecasts

No.25 On the Atmospheric Factors Affecting the Levantine Sea

No.26 Tropical Influences on Stationary Wave Motion in Middle and High Latitudes